[redacted] CONFIDENTIAL

NASA TM X-393

NASA TM X-393

TECHNICAL MEMORANDUM
X-393

AERODYNAMIC CHARACTERISTICS OF A BLUNT HALF-CONE ENTRY CONFIGURATION AT MACH NUMBERS FROM 3 TO 6

By Michael F. Sarabia

Ames Research Center
Moffett Field, Calif.

[redacted]

[redacted] DOCUMENT [redacted] UNCLASSIFIED

[redacted]

DATE of DOC.
Oct. 1960

NATIONAL AERONAUTICS AND SPACE ADMINISTRATION
WASHINGTON

lM

[redacted]

NATIONAL AERONAUTICS AND SPACE ADMINISTRATION

TECHNICAL MEMORANDUM X-393

AERODYNAMIC CHARACTERISTICS OF A BLUNT HALF-CONE ENTRY CONFIGURATION AT MACH NUMBERS FROM 3 TO 6*

By Michael F. Sarabia

SUMMARY

Experimental and theoretical studies were conducted with a configuration similar to the one described in NASA Memorandum 10-2-58A. The configuration is basically half of a blunt 30° circular cone with a trimmed lift-drag ratio of about 0.5 at supersonic speeds. Two sets of controls were investigated with this configuration. One set, similar to the one described in the forementioned reference, consisted of four trailing-edge flaps of aspect ratio 0.6. The second set consisted of two horizontal flaps of aspect ratio 1 for pitch control, and two vertical flaps of aspect ratio 0.6 for yaw control.

The results of the tests indicated: (1) The configuration is stable at Mach numbers from 3 to 6 and angles of attack ranging from -18° to +18°. (2) The first set of controls described can provide longitudinal, lateral, and directional control at angles of attack near zero; however, the aerodynamic cross coupling at angles other than zero could not be eliminated. (3) The second set of controls studied can provide longitudinal and directional control through a large range of angles of attack with little cross coupling but has no provisions for direct roll control. Roll control would, therefore, have to be provided by other means, for example, reaction jets.

INTRODUCTION

The motion and heating of near-earth satellites during entry into the earth's atmosphere have been thoroughly investigated in a number of studies (see, e.g., refs. 1 to 4). As a result of these studies, the

[redacted]

problems associated with atmosphere entry are now well recognized. In current investigations (refs. 1, 5, and 6) attention is often directed toward the study of configurations which appear attractive as entry vehicles. In reference 1 such a configuration was suggested and a preliminary evaluation of its characteristics was presented. The configuration is basically half of a blunt 30° circular cone with four trailing-edge flap-type controls. Further studies of the characteristics of this configuration have been made to provide additional information on its performance and stability, its control characteristics, and the pressure distribution over the body and control surfaces. The results of the investigation are the subject of this report.

A 2 3 0

NOTATION

A base area of vehicle, $1.26\,l^2$

C_D drag coefficient, $\frac{\text{drag}}{q_\infty A}$

C_L lift coefficient, $\frac{\text{lift}}{q_\infty A}$

C_l rolling-moment coefficient, $\frac{\text{rolling moment}}{q_\infty Ad}$ (body axes)

C_m pitching-moment coefficient, $\frac{\text{pitching moment}}{q_\infty Al}$ (body axes)

C_n yawing-moment coefficient, $\frac{\text{yawing moment}}{q_\infty Ad}$ (body axes)

C_p pressure coefficient, $\frac{p-p_\infty}{q_\infty}$

C_Y side-force coefficient, $\frac{\text{side force}}{q_\infty A}$ (body axes)

d base diameter of vehicle

l length of vehicle

M Mach number

p static pressure

p_∞ free-stream static pressure

q_∞ free-stream dynamic pressure

α angle of attack (measured with respect to the top surface)

β angle of sideslip

Δ incremental change due to control deflection

δ_{a_l} deflection of the lower control as aileron (control set I)

δ_{a_u} deflection of the upper control as aileron (control set I)

A
2
3
0

δ_{e_l} deflection of the lower controls as elevators (control set I)

δ_{e_u} deflection of the upper controls as elevators (control set I)

δ_l deflection of the lower control (control set II)

δ_u deflection of the upper control (control set II)

δ_r deflection of the side control (control set II)

Note: At zero deflection, control is normal to the body base and positive deflections are outward into the air stream.

Subscript

β derivative with respect to angle of sideslip

APPARATUS AND TESTS

The configuration tested is slightly more than half of a blunt 30° circular cone with a flat section which has circular leading edges mounted on top for added depth. A dimensioned three-view sketch and a photograph of the model tested are shown in figures 1 and 2, respectively.

The configuration studied included a set of four trailing-edge flaps with aspect ratios of 0.6 (control set I) similar to the set described in reference 1. This first control set is shown in figures 1 and 2. Additional studies were made with a set of trailing-edge flaps (control set II) consisting of two horizontal flaps of aspect ratio 1 and two vertical flaps of aspect ratio 0.6. This second set of controls is shown in figure 3.

The tests were conducted in the Ames 10- by 14-Inch Supersonic Wind Tunnel (ref. 7) at Mach numbers 3, 4, 5, and 6 and angles of attack ranging from -18° to $+18^\circ$. This range of angles was obtained in part by rotation of the support system through $\pm 4^\circ$ and in part by the use of stings bent to angles of 0°, 7°, and 14°. The lateral-directional characteristics were measured at sideslip angles from -4° to $+4^\circ$ at angles of attack of approximately -7°, 0°, 7°, and 14°. The controls were tested at 0°, 30°, and 60° deflection (for zero control deflection the controls are normal to the body base). Test Reynolds numbers, based on body diameter, are given in the following table:

Mach number	Reynolds number, million
3	0.43
4	1.82
5	.79
6	.38

The forces and moments on the model were measured with a six-component strain-gage balance. The model was supported from the base by the balance assembly which was shrouded to eliminate any direct aerodynamic loads on the balance.

All force and moment coefficients are referenced to the body base area. The pitching-moment coefficients are referenced to body length and the yawing- and rolling-moment coefficients to body base diameter.

For the forebody and control pressure surveys the model was supported from the base and for the base pressure survey the model was supported from the top. Photographs of the models used in the pressure distribution tests are shown in figure 4. The pressure coefficients were evaluated from data taken with conventional dibutylphthalate and mercury manometers.

Accuracy of the experimental results was affected by uncertainties in the measured values of the pressures, forces, and moments and in the determination of stream static and dynamic pressures and angles of attack and sideslip. The combination of these uncertainties resulted in estimated maximum errors in the test results as shown in the following table:

M	3	4	5	6
α, β	0.1°	0.1°	0.1°	0.1°
C_L, C_Y	0.008	0.008	0.010	0.010
C_D	0.010	0.010	0.020	0.020
L/D	0.015	0.015	0.020	0.020
C_l	0.003	0.003	0.004	0.004
C_m, C_n	0.003	0.003	0.005	0.005
C_p	0.015	0.015	0.020	0.020

[redacted]

It should be noted that, for the most part, the test results presented are in error by less than these estimates.

RESULTS AND DISCUSSION

Experimental results for the study configuration shown in reference 1 indicated a decrease in longitudinal static stability at positive angles of attack; this decrease was believed due to overexpansion of the flow in the region of the nose-cone juncture. For this reason the profile was modified from the hemisphere-cone used in reference 1. The modification, which is shown in figure 5, was selected to give the body profile continuous curvature in the transition region from the spherical nose to the conical body. The change in profile is small as is shown in figure 5. The modification resulted in improved pitching-moment characteristics as shown in figure 6. In this figure the moment characteristics of the configuration before and after modification of the profile are compared. All of the subsequent experimental results presented herein were obtained with the modified body-nose profile.

The longitudinal aerodynamic characteristics of the configuration were estimated with the aid of Newtonian impact theory for the nose and conical surface and two-dimensional shock-expansion theory for the top surface. The base-pressure coefficient was assumed to be equal to 0.7 of the vacuum pressure coefficient. The lateral-directional derivatives and control characteristics were estimated with the aid of Newtonian impact theory. The results of these calculations are presented together with the experimental results.

Performance and Longitudinal Stability

The variations with angle of attack of lift, drag, lift-drag ratio, and pitching moment of the study configuration with all flaps of control set I at zero deflection (90° relative to the base) at Mach numbers 3, 4, 5, and 6 are shown in figure 7. At these Mach numbers the configuration was stable and was trimmed at an angle of attack of about 2°. The lift coefficient at this attitude was about 0.4 and the lift-drag ratio was about 0.5. As noted earlier, these data were obtained with the aid of bent stings. For this reason, several tests were made at each Mach number to cover the complete range of angles of attack. The data presented in figure 7 were obtained by a combination of these runs. This procedure accounts for the steplike scatter in the pitching-moment results, particularly at test Mach numbers of 5 and 6.

It may be seen that the estimated values of lift and drag are in close agreement with the measured values over the test ranges of Mach numbers and angles of attack. In figures 7(c) and 7(d), $M = 5$ and $M = 6$, respectively, the estimates obtained with the aid of simple impact theory ($M = \infty$) are also shown. For these estimates the pressure coefficients are assumed to be zero for all vehicle surfaces which do not "see" the oncoming flow. The primary difference between the estimated drag value at $M = 5$ and 6 and the estimate for $M = \infty$ is the base drag which is assumed equal to $1/M^2$. The lift coefficients estimated for $M = 5$ and 6 differ from the calculated values for $M = \infty$ in the contribution of the pressures acting on the flat top. In the former estimate these pressures were estimated with the aid of shock-expansion theory, while in the latter case, they were calculated with the aid of Newtonian impact theory. It is evident that for these Mach numbers, better agreement with experimental results is obtained with results based on the calculations which include estimates of the pressures on the base.

The estimated trim angle of attack agrees well with the measured values. However, the changes in the measured pitching moment with angle-of-attack variation are greater than estimated. The variation of measured pitching moment with angle of attack may be seen to approach the estimated variation with increasing Mach number. In the calculation of the pitching moments the contributions of the pressures acting on the top surface and the base were negligible since both resultant forces act very nearly through the moment reference center. For this reason, the estimated pitching moments are essentially the same for all Mach numbers.

Lateral-Directional Stability

The effect of variations of angle of attack and of Mach number on the lateral-directional-stability parameters, C_{n_β}, C_{Y_β}, and C_{l_β}, are shown in figure 8. The results show that the configuration is statically stable at all Mach numbers over the angle-of-attack range investigated. It is also evident that variations of test Mach number and of angle of attack have very little effect on the stability levels. The agreement between the measured values and those estimated for $M = \infty$ is fairly good.

Control Effectiveness

The characteristics of control set I with the body at an angle of 0° are shown in figure 9 and table I. The decrease in effectiveness

of the upper controls with increasing Mach number is partly associated with the decrease of wind-tunnel Reynolds number. Because of this decrease, shock-wave boundary-layer interaction increases. This interaction manifests itself in an increase in boundary-layer thickness. Portions of the control inside the boundary layer experience lower pressures than the exposed portions. This interaction is partially alleviated by a gap (0.021 l) between the body base and the control hinge line. At a deflection angle of 60° and a Mach number of 4 the pitching moment in figure 9 is about 10 percent of the control contribution greater than the moment presented in reference 1. This increment is due to the gap added for the present tests. The increase in effectiveness of the lower controls at large control deflections with increasing Mach number is associated with changes in the flow about the controls discussed in the presentation of the pressure-survey results. The effect of angle of attack on the pitch control characteristics is shown in figure 10.

From the control characteristics shown in figures 9 and 10, tables I and II, and the body characteristics, estimates have been made of the ability of control set I to trim the study vehicle over a range of lift-drag ratios. The results are tabulated below:

No.	L/D	C_D	α_{trim}	δ_{e_u}	δ_{e_l}
1	0.37	1.04	15°	30°	0°
2	0.50	0.72	2°	0°	0°
3	0	0.53	-18°	0°	25°
4	0.46	0.75	0°	30°	18°
5	0.32	0.97	0°	60°	45°
6	0.22	1.25	-2°	90°	65°

Two methods of varying the lift-drag ratio were considered. With the first method, the lift-drag ratio was varied in the conventional manner by varying the trim angle of attack (numbers 1, 2, and 3). With the second method, the controls were employed as drag brakes while the trim angle of attack was maintained approximately constant at 0° (numbers 2, 4, 5, and 6). From these tabulated results, it is apparent that control set I provides for a reasonably wide variation of L/D by either attitude control or drag modulation.

It is also apparent from figure 9, however, that when the upper controls are used singly as ailerons, large pitching and yawing as well as rolling moments are produced. It was found (see ref. 1) that this cross coupling could be eliminated for small control deflections at zero angle of attack by appropriately gearing opposite controls (e.g., the lower left and the upper right) and thus a nearly pure rolling moment could be produced. Pure yawing moments could be produced by deflecting a lower control and cancelling the undesired moments by appropriately gearing the two upper controls.

Since relative deflection of the controls required to eliminate undesired moments is a function of angle of attack, as indicated in figure 10, and of control deflection, the cancellation of the undesired moments for large control deflections or at angles of attack other than zero requires corrections in the deflection of the controls in addition to the simple gearing. A simple method to eliminate control cross coupling aerodynamically over the ranges of angles of attack and control deflections was not found. For this reason, an alternate control system was also studied briefly.

The alternate system (control set II) consisted of single upper and lower flaps for longitudinal control and single flaps at either side of the body base for yaw control. No provision was made for aerodynamic control about the longitudinal axis. It would be anticipated that a reaction-type system might be used for roll control. With the elimination then of the differential deflection of the pairs of controls that is required for yaw and roll control with control set I, it would be expected that only minor interactions would occur for the alternate system.

A230

The characteristics of control set II at an angle of attack of 0° are shown in figure 11 and table I. As shown in figure 11 the side flaps of control set II can provide yawing moments with only small accompanying pitching moments. There is a small pitching-moment contribution because the control drag acts along a line vertically displaced from the moment reference center. This cross coupling could be eliminated by a small change in the flap location. Control set II can be used to vary the lift-drag ratio by varying the trim angle of attack or by increasing the drag at a trimmed angle of attack near to 0°. An estimate of the range of lift-drag ratios possible with the two methods was made. Newtonian impact theory was used to estimate the control characteristics and experimental data at $M = 3$ were used for the body characteristics. The results are presented in figure 12. The ranges of variation of lift-drag ratio may be seen to be similar to those obtainable with control set I.

Pressure Survey

Body.- The results of the pressure survey on the forebody of the study configuration at an angle of attack of 0° and Mach numbers of 3, 4, 5, and 6 are shown in figure 13. Comparison is made with estimated pressure coefficients obtained with Newtonian impact theory. In general, the agreement between the estimated and experimental results is good aft of the nose. In this case, agreement at the nose would probably be better if impact theory were modified to give the correct pressure coefficient at the stagnation point. In figure 14 the effect of angle

of attack on the body pressure coefficients is indicated. The base pressure coefficients with the body at an angle of attack of 4° are shown in figure 15 together with the value estimated assuming the pressure coefficient to be 0.7 of the vacuum pressure coefficient.

Controls.- Pressure coefficients on the controls (control set I) at a body angle of attack of 0° are shown in figures 16 and 17. At high deflection angles, pressure coefficients up to about 5 were found. These values are much higher, of course, than those predicted with Newtonian impact theory. These high pressures are a result of the multiple shock-wave compression of the flow and are, therefore, higher than the pressure at the nose stagnation point. The effect of this multiple shock-wave type of compression increases with increasing Mach number as evidenced by the increase in peak pressure coefficient with increasing Mach number shown in figures 16 and 17. The shock-wave patterns about the controls are shown in figure 18. Pressures on the upper control are also affected by shock-wave boundary-layer interaction, as can be seen by the low value of the pressure coefficient at station $y/a = 0.15$. This effect also increases with increasing Mach number primarily because of the decrease in test Reynolds number. The latter effect seems to predominate with the upper controls, for the effectiveness of these controls decreases while that of the lower controls increases with Mach number, as can be seen in figure 9.

SUMMARY OF RESULTS

An investigation has been made of the performance, stability, and control characteristics of a high-lift, high-drag, satellite-entry configuration similar to that proposed previously in NASA Memorandum 10-2-58A. Tests were conducted at Mach numbers from 3 to 6, at angles of attack from -18° to $+18^\circ$, at angles of sideslip up to 4°, and for control deflections up to 90°. The results of this investigation are as follows:

1. The configuration studied is longitudinally, directionally, and laterally stable at all test angles of attack and Mach numbers. With controls undeflected the vehicle trims at approximately 0° angle of attack and a lift-drag ratio of 0.5. Either of the two control sets investigated provides trim at lift-drag ratios from about 0 to about 0.5.

2. For the first control set studied, lateral-directional and longitudinal control moments are cross coupled. Cross coupling can be eliminated at zero angle of attack by the proper deflection of the controls. No method was found for eliminating cross coupling aerodynamically over a range of angles of attack.

3. The second control set produces yawing and pitching moments largely independent of each other. This set of controls requires that the rolling moments be produced by some other means.

Ames Research Center
National Aeronautics and Space Administration
Moffett Field, Calif., June 29, 1960

A 2 3 0

REFERENCES

1. Eggers, A. J., Jr., and Wong, T. J.: Re-entry and Recovery of Near-Earth Satellites, With Particular Attention to a Manned Vehicle. NASA MEMO 10-2-58A, 1958.

2. Eggers, A. J., Jr.: The Possibility of a Safe Landing. Ch. 13, Space Technology. John Wiley and Sons, Inc., 1959.

3. Chapman, D. R.: An Approximate Analytical Method for Studying Entry Into Planetary Atmospheres. NASA TR R-11, 1959. (Supersedes NACA TN 4276)

4. Slye, Robert E.: An Analytical Method for Studying the Lateral Motion of Atmosphere Entry Vehicles. NASA TN D-325, 1960.

5. Savage, Howard F., and Tinling, Bruce E.: Subsonic Aerodynamic Characteristics of Several Blunt, Lifting, Atmospheric-Entry Shapes. NASA MEMO 12-24-58A, 1958.

6. Hassell, James L., Jr.: Investigation of the Low-Subsonic Stability and Control Characteristics of a 1/3-Scale Free-Flying Model of a Lifting-Body Type Reentry Configuration. NASA TM X-297, 1960.

7. Eggers, A. J., Jr., and Nothwang, George J.: The Ames 10- by 14-Inch Supersonic Wind Tunnel. NACA TN 3095, 1954.

TABLE I.- CONTROL EFFECTIVENESS AT $\alpha = 0^{\circ}$;

CONTROL SET I

δ_{a_l}	δ_{a_u}	M	ΔC_L	ΔC_D	ΔC_m	ΔC_n	ΔC_l
0°	30°	3	-0.0215	0.0158	0.0165	0.0032	0.0050
		4	-.0201	.0194	.0093	.0043	.0047
		5	-.0194	.0144	.0079	.0047	.0030
		6	-.0194	.0180	.0122	.0057	.0047
0°	60°	3	---	.0574	.0540	.0194	.0140
		4	-.0488	.0539	.0452	.0179	.0131
		5	-.0467	.0582	.0410	.0165	.0101
		6	-.0467	.0388	.0295	.0155	.0118
30°	0°	3	.0273	.0323	-.0280	-.0136	.0036
		4	.0251	.0223	-.0273	-.0129	.0018
		5	.0251	.0323	-.0244	-.0136	.0038
		6	.0310	.0230	-.0205	---	---
60°	0°	3	.0359	.1243	-.0865	-.0446	.0030
		4	.0467	.1320	-.0940	-.0467	.0029
		5	.0560	.1393	-.1052	-.0470	.0026
		6	.0660	.1600	-.1110	-.0513	---

TABLE I.- CONTROL EFFECTIVENESS AT $\alpha = 0^\circ$;

CONTROL SET II - Concluded

δ_l	δ_u	δ_r	M	ΔC_L	ΔC_D	ΔC_m	ΔC_n	ΔC_l
0°	30°	0°	3	-0.0445	0.0452	0.0467	0	0
			4	-.0323	.0309	.0330	0	0
			5	-.0230	.0223	.0223	0	0
			6	-.0180	.0273	.0230	0	0
0°	60°	0°	3	-.0898	.0890	.0840	0	0
			4	-.0768	.0696	.0790	0	0
			5	-.0617	.0632	.0696	0	0
			6	-.0539	.0639	.0811	0	0
30°	0°	0°	3	.0546	.0747	-.0664	0	0
			4	.0574	.0610	-.0646	0	0
			5	.0517	.0553	-.0574	0	0
			6	.0682	.0589	-.0639	0	0
60°	0°	0°	3	.1106	.2761	-.2097	0	0
			4	---	---	---	---	---
			5	.1099	.2599	-.2104	0	0
			6	---	---	---	---	---
0°	0°	30°	3	0	.0538	.0025	.0244	0
			4	0	.0438	.0022	.0237	0
			5	0	.0359	.0061	.0223	-.0032
			6	-.0043	.0108	.0079	.0287	-.0090
0°	0°	60°	3	-.0250	.1400	.0215	.0998	0
			4	---	---	---	---	---
			5	-.0151	.1508	.0140	.1106	0
			6	-.0402	.1178	.0198	.1041	-.0086

TABLE II.- EFFECT OF CONTROL DEFLECTION ON PERFORMANCE; CONTROL SET I

δ_{e_u}	δ_{e_l}	M	α	C_L	L/D	C_m	δ_{e_u}	δ_{e_l}	M	α	C_L	L/D	C_m
30°	15°	3	-3.9	0.298	0.393	0.0359	60°	30°	4	-3.9	0.236	0.280	0.1085
			-2.9	.318	.405	.0275				-2.8	.257	.300	.0920
			-1.9	.334	.425	.0187				-1.8	.276	.320	.0778
			-.8	.345	.438	.0115				-.8	.296	.338	.0632
			.2	.370	.445	.0087				.2	.313	.352	.0517
			1.2	.383	.451	-.0087				1.2	.331	.368	.0381
			2.2	.399	.460	-.0115				2.2	.348	.381	.0259
			3.2	.412	.465	-.0180				3.2	.362	.390	.0129
			4.2	.427	.470	-.0244				4.3	.373	.397	.0043
		4	-3.9	.279	.410	.0330			5	-3.9	.230	.275	.1135
			-2.8	.298	.423	.0251				-2.9	.254	.304	.0947
			-1.8	.314	.438	.0194				-1.9	.276	.325	.0789
			-.8	.332	.450	.0106				-.9	.297	.346	.0646
			.2	.346	.460	.0057				.1	.316	.365	.0540
			1.2	.362	.472	0				1.1	.334	.382	.0402
			2.2	.375	.476	-.0057				2.1	.350	.395	.0266
			3.2	.386	.480	-.0122				3.1	.365	.402	.0158
			4.2	.397	.482	-.0169				4.1	.380	.410	.0029
		5	-3.9	.282	.433	.0287			6	-4	.241	.255	.1250
			-2.9	.298	.452	.0201				-3	.266	.280	.0983
			-1.9	.317	.464	.0133				-2	.292	.310	.0740
			-.9	.334	.476	.0079				-1	.313	.325	.0560
			.1	.349	.487	.0014				0	.334	.350	.0295
			1.1	.363	.492	-.0036				1	.358	.365	.0126
			2.1	.377	.497	-.0112				2	.374	.378	-.0014
			3.1	.390	.501	-.0172				3.1	.392	.390	-.0187
			4.1	.402	.503	-.0226				4.1	.406	.395	-.0323
		6	-4	.304	.433	.0259	90°	65°	3	-3.9	.275	.210	.0103
			-3	.322	.452	.0172				-1.8	.302	.216	-.0027
			-2	.341	.466	.0086				-.9	.309	.218	-.0125
			-1	.360	.480	0				.1	.322	.221	-.0206
			0	.375	.490	-.0036				1.1	.327	.223	-.0305
			1	.391	.495	-.0129				2.1	.332	.225	-.0374
			2.1	.404	.495	-.0183				3.1	.340	.226	-.0446
			3.1	.416	.496	-.0257				4.1	.345	.227	-.0538
			4.1	.427	.496	-.0323							
60°	30°	3	-3.9	.260	.265	.1090			5	-2.9	.272	.220	.0122
			-2.9	.280	.295	.0948				-1.9	.283	.225	-.0057
			-1.9	.300	.312	.0884				-.9	.294	.232	-.0137
			-.8	.318	.326	.0675				.1	.309	.241	-.0309
			.2	.334	.337	.0596							
			1.2	.350	.350	.0460							
			2.2	.365	.363	.0316							
			3.2	.380	.371	.0208							
			4.2	.395	.379	.0079							

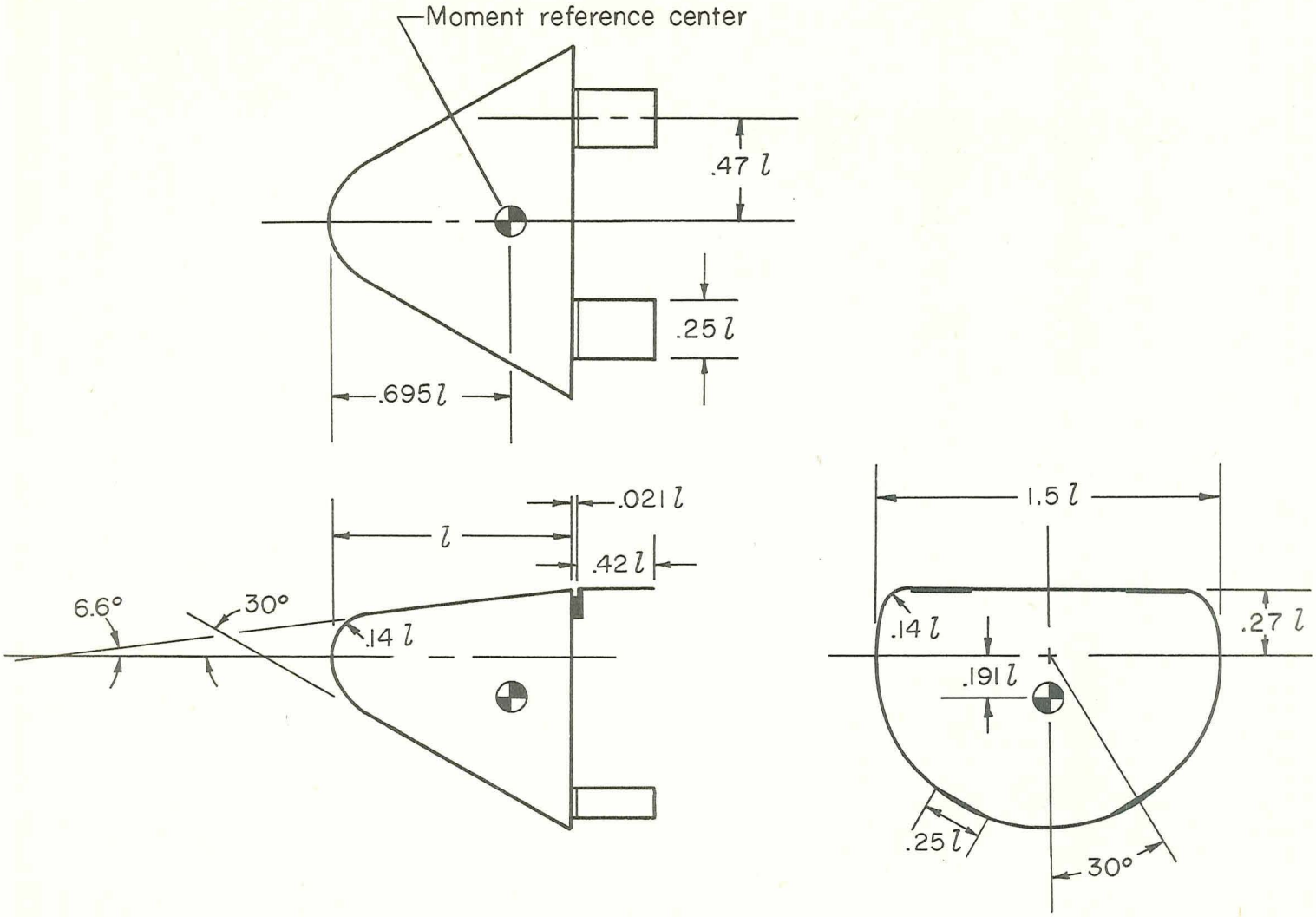

Figure 1.- Study configuration; control set I.

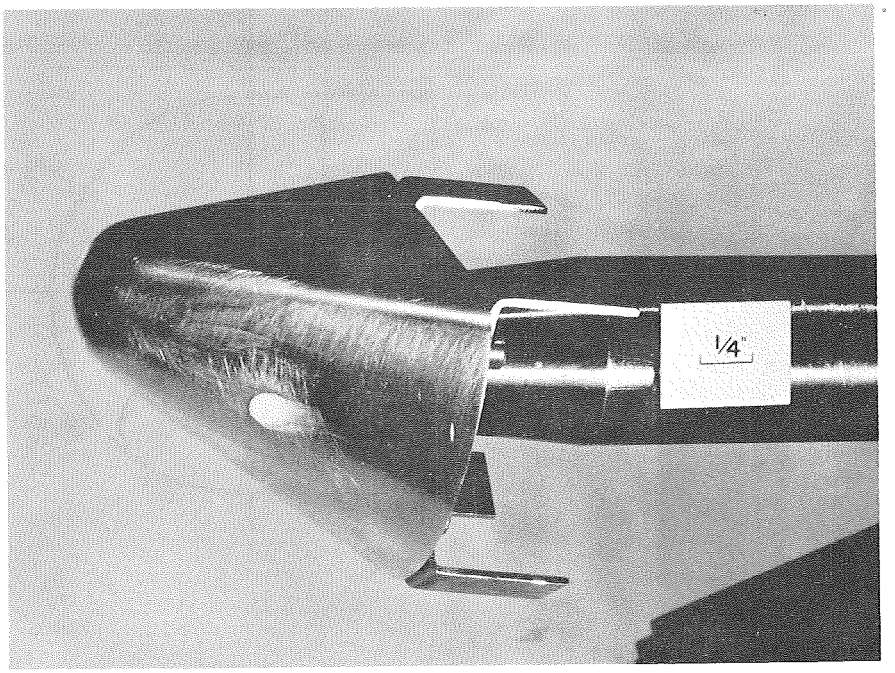

A-26831

Figure 2.- Model tested with control set I.

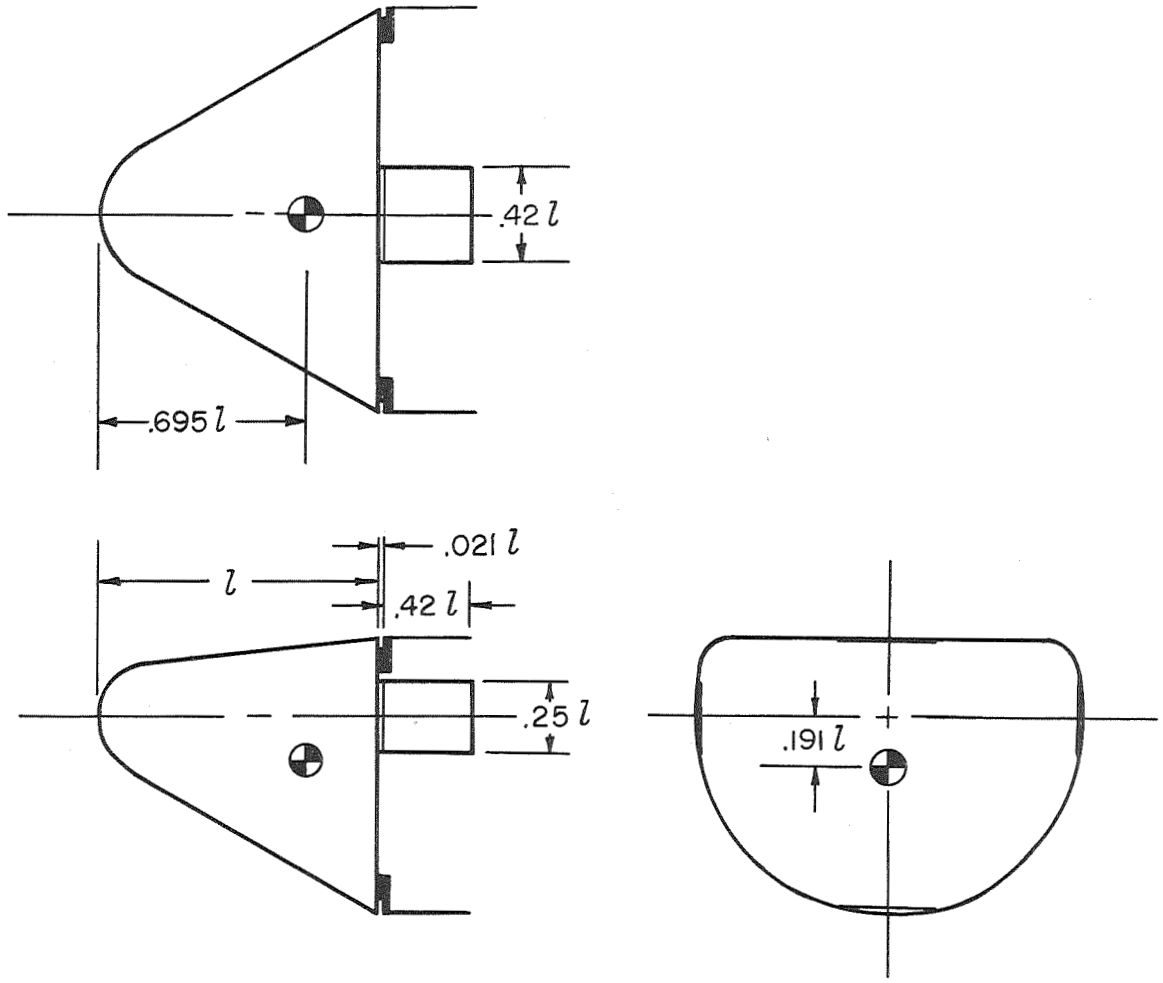

Figure 3.- Study configuration; control set II.

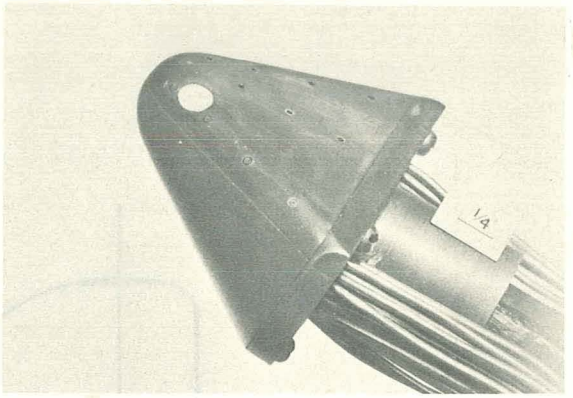

(a) Forebody pressure model. A-26829

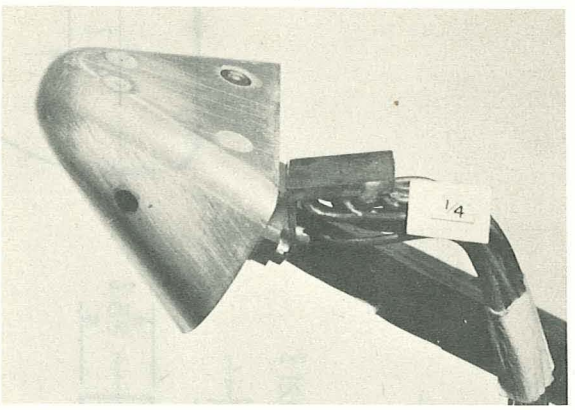

(b) Control pressure model. A-26830

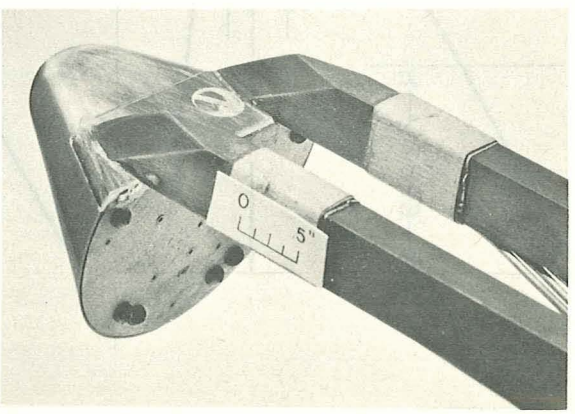

(c) Base pressure model. A-26392

Figure 4.- Pressure survey models.

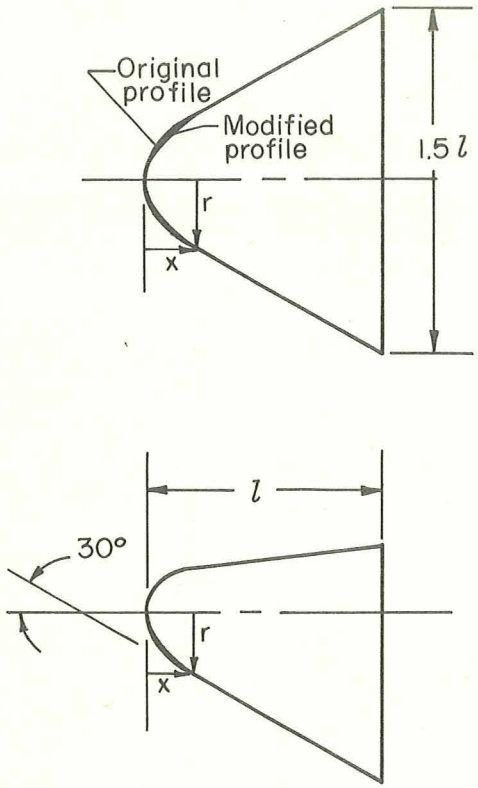

x/l	Original profile r/l	Modified profile r/l
.0047	.0529	.0529
.0177	.1014	.1014
.0234	.1162	.1162
.0334	.1376	.1362
.0434	.1555	.1523
.0534	.1710	.1664
.0668	.1889	.1827
.0834	.2077	.1998
.1001	.2239	.2147
.1168	.2378	.2285
.1335	.2503	.2415
.1669	.2700	.2652
.2003	.2892	.2869
.2336	.3085	.3076
.2670	.3278	.3273
.3338	.3663	.3663
.4005	.4048	.4048
1.000	.7510	.7510

Figure 5.- Modification of the configuration studied.

A230

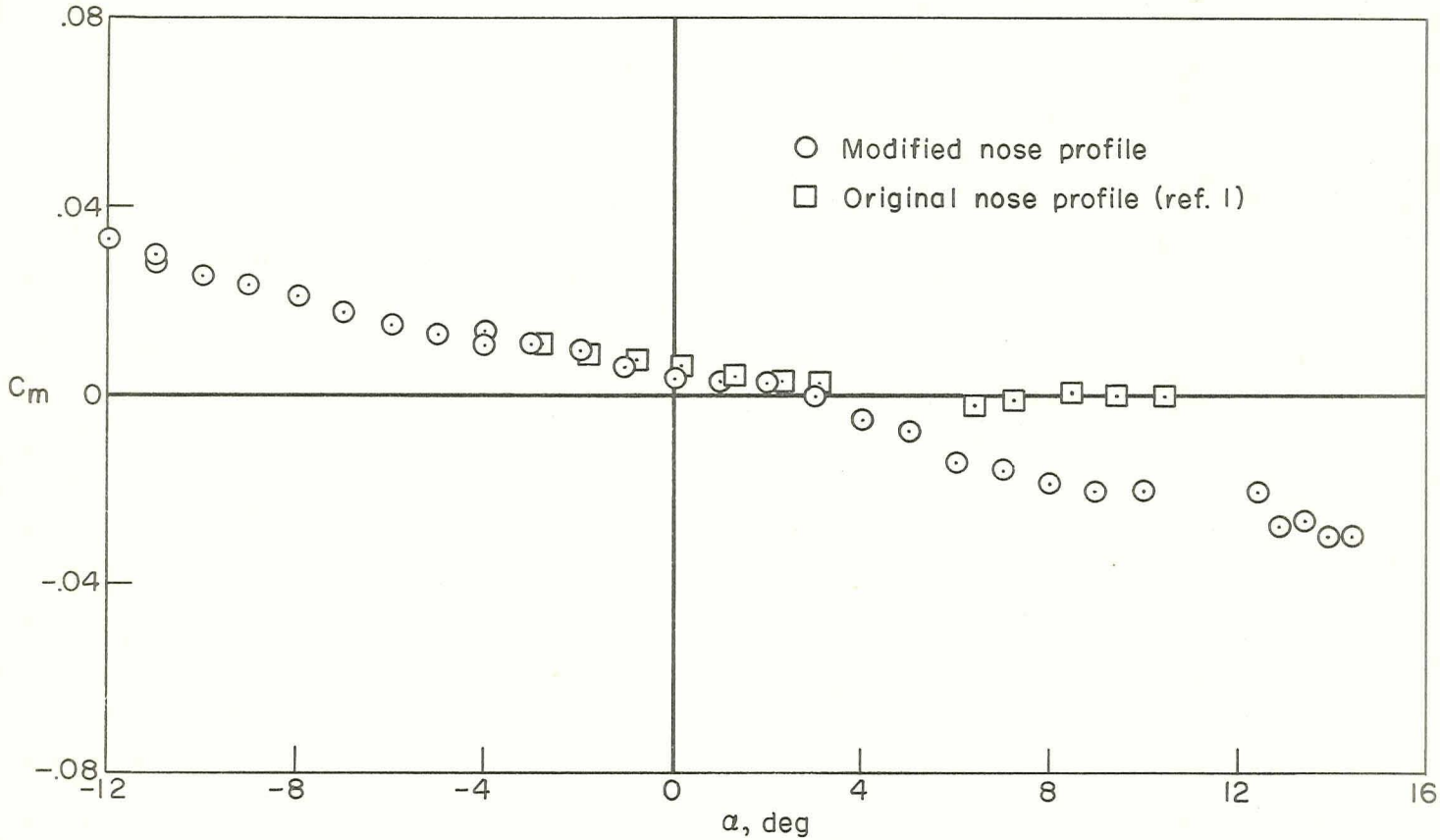

Figure 6.- Pitching moments of study configuration at M = 4; control set I undeflected.

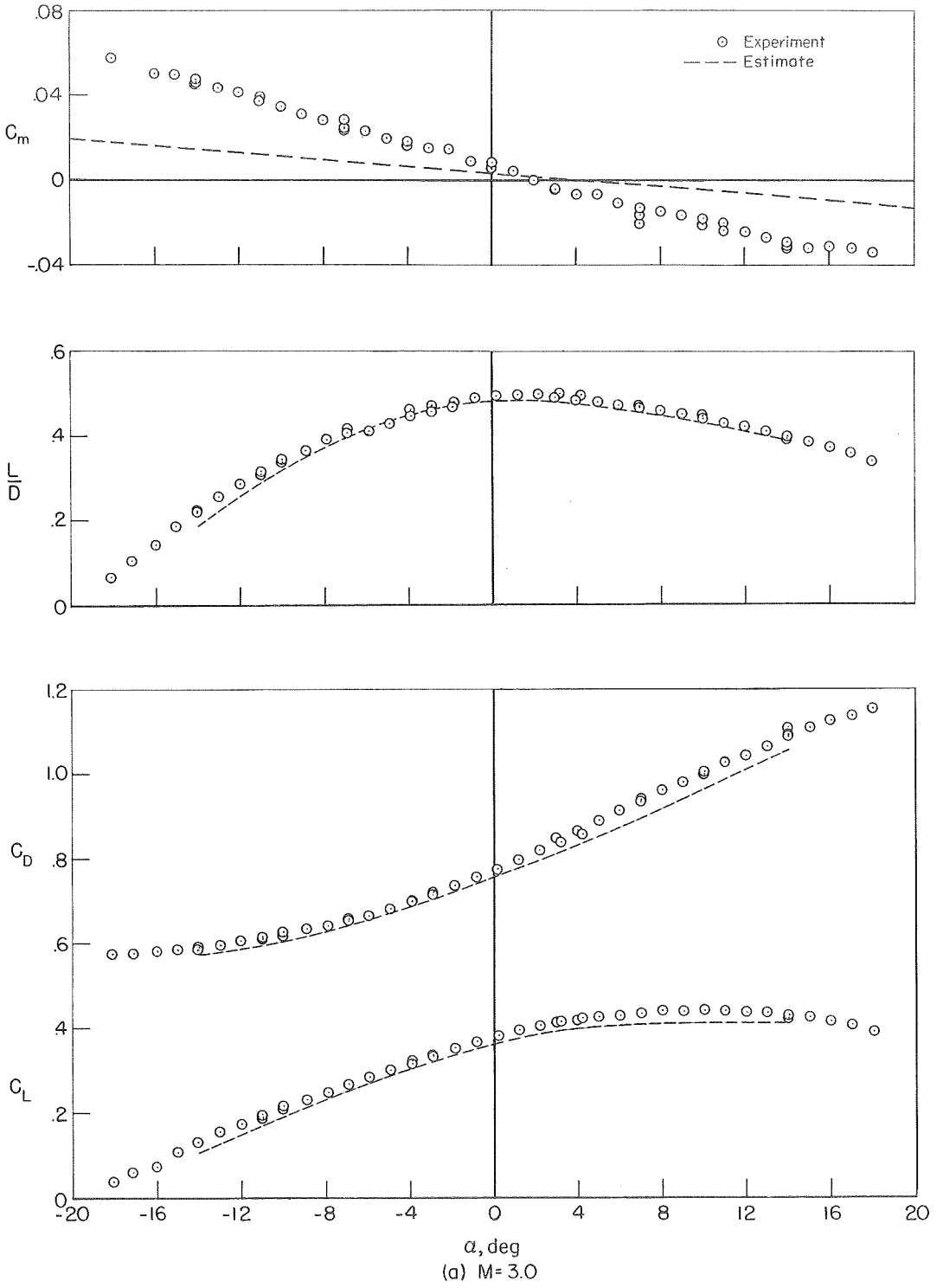

Figure 7.- Longitudinal characteristics of the study configuration; control set I undeflected.

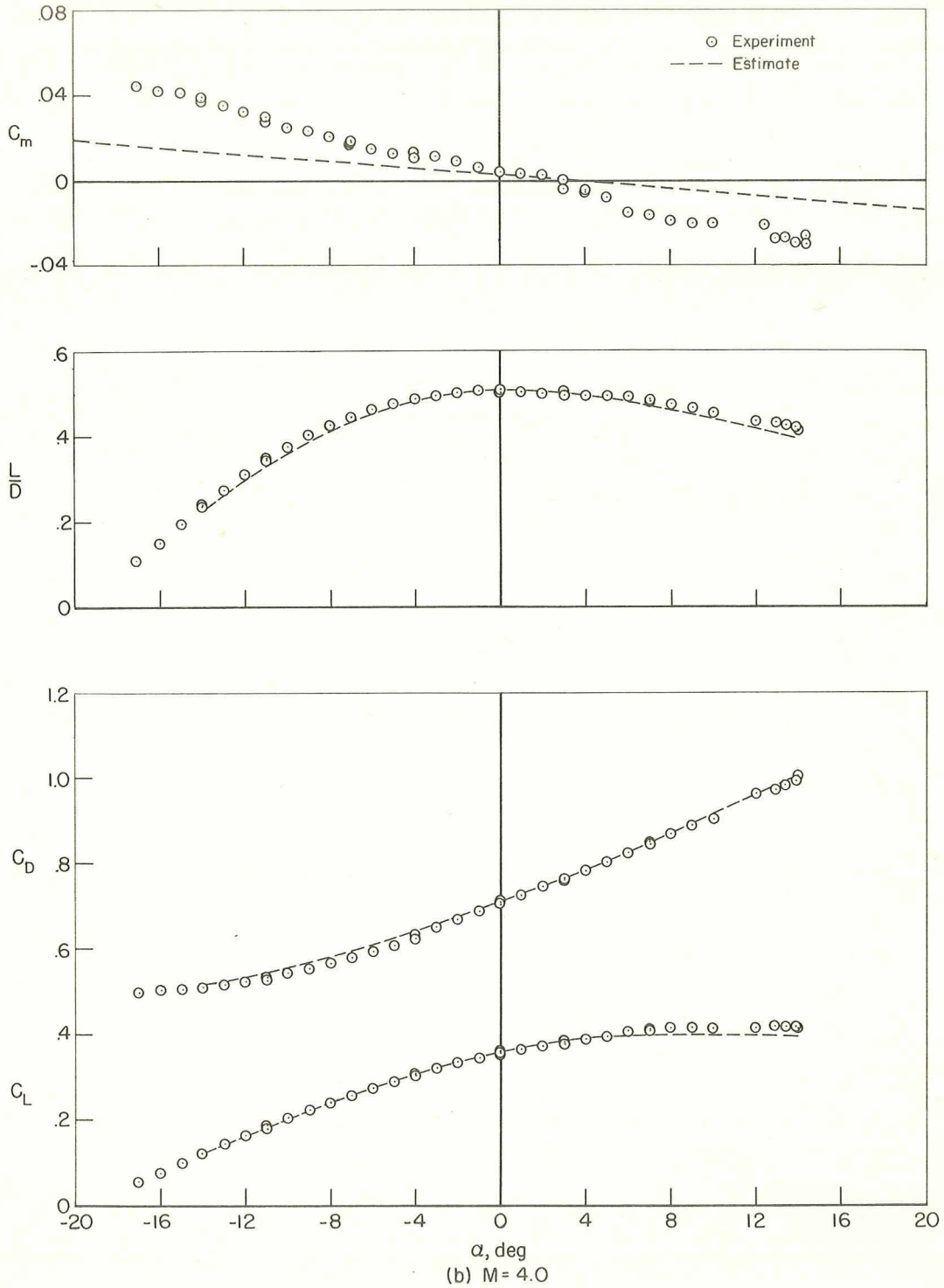

(b) M = 4.0

Figure 7.- Continued.

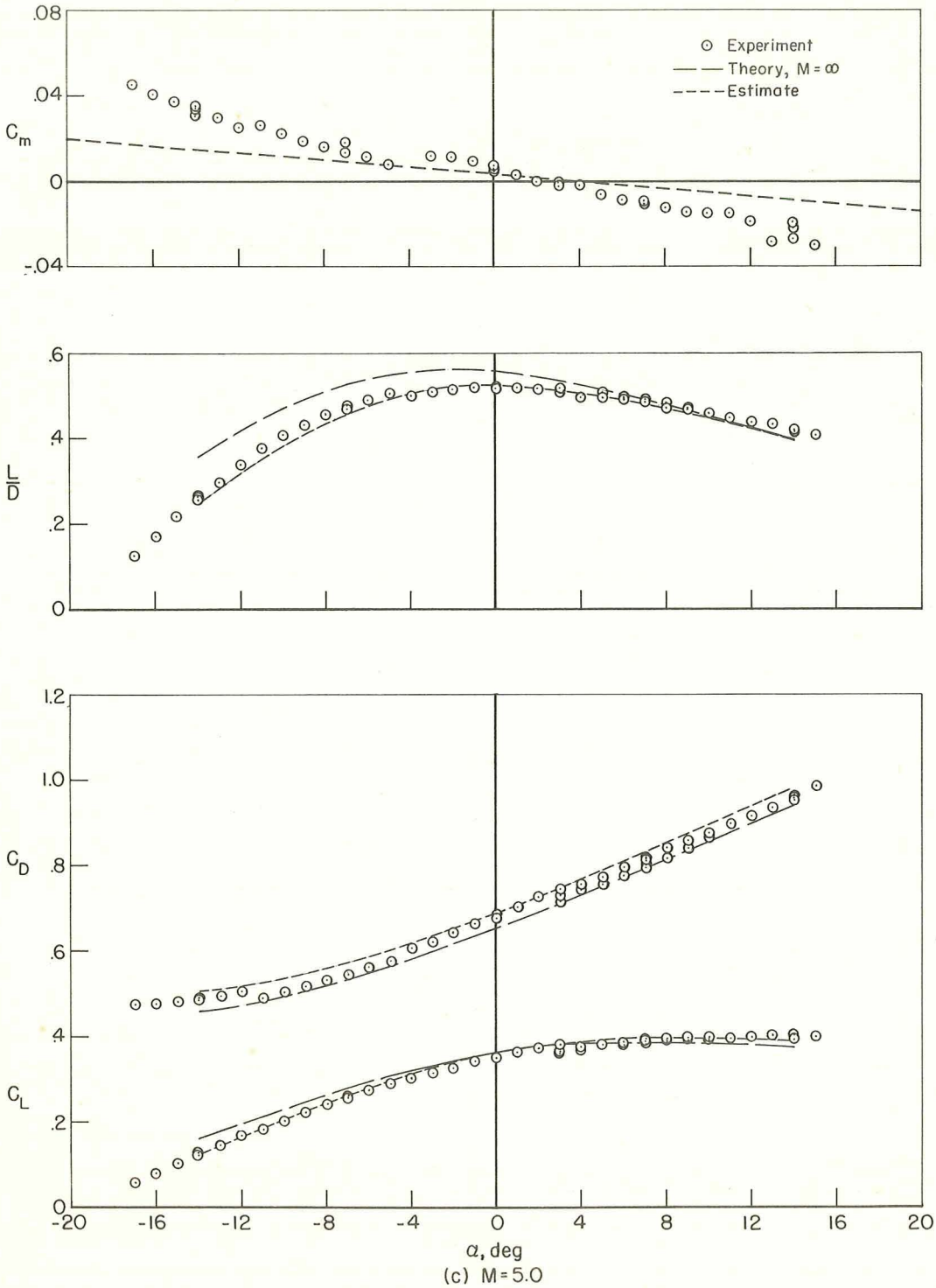

(c) M=5.0

Figure 7.- Continued.

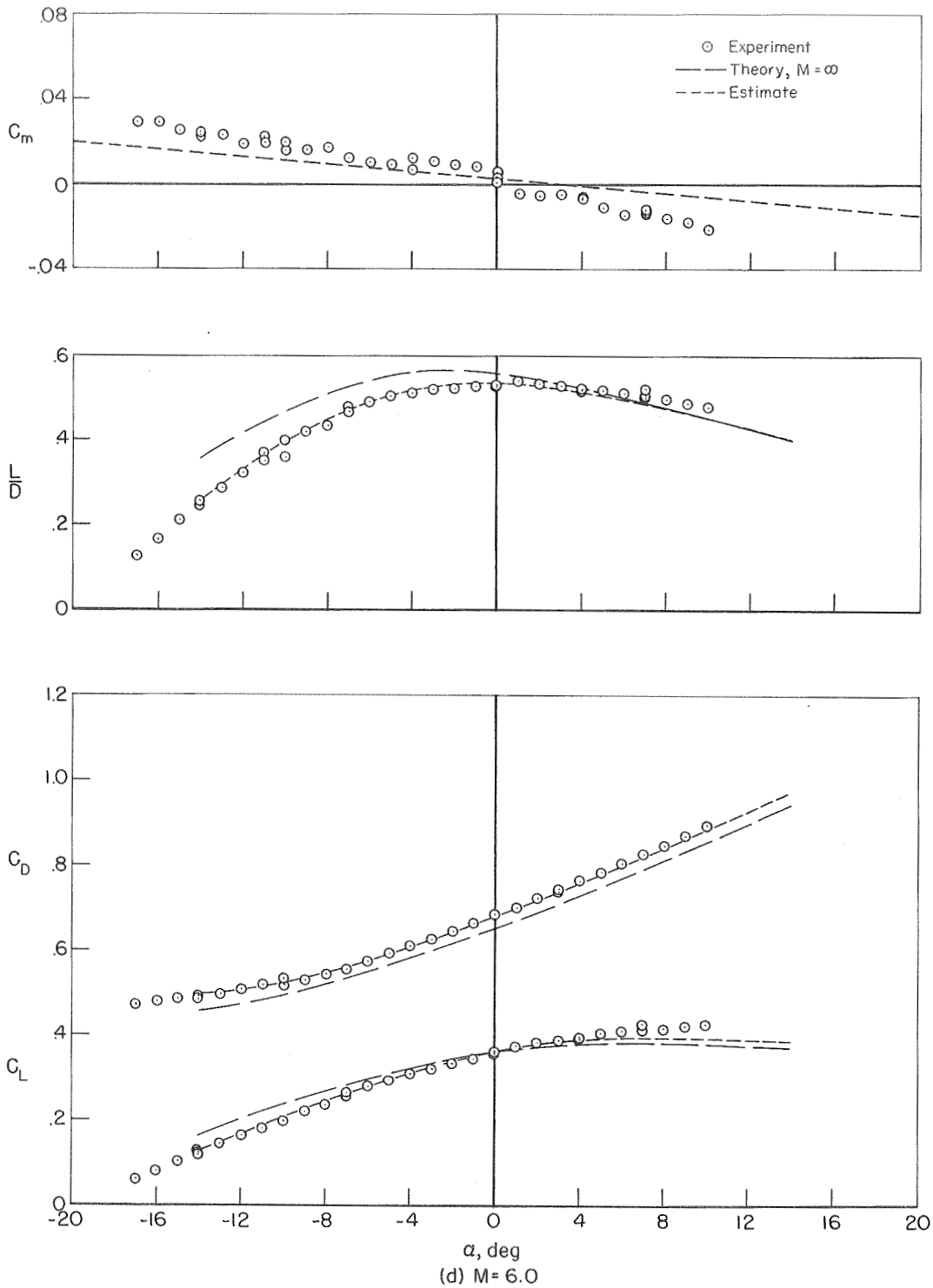

Figure 7.- Concluded.

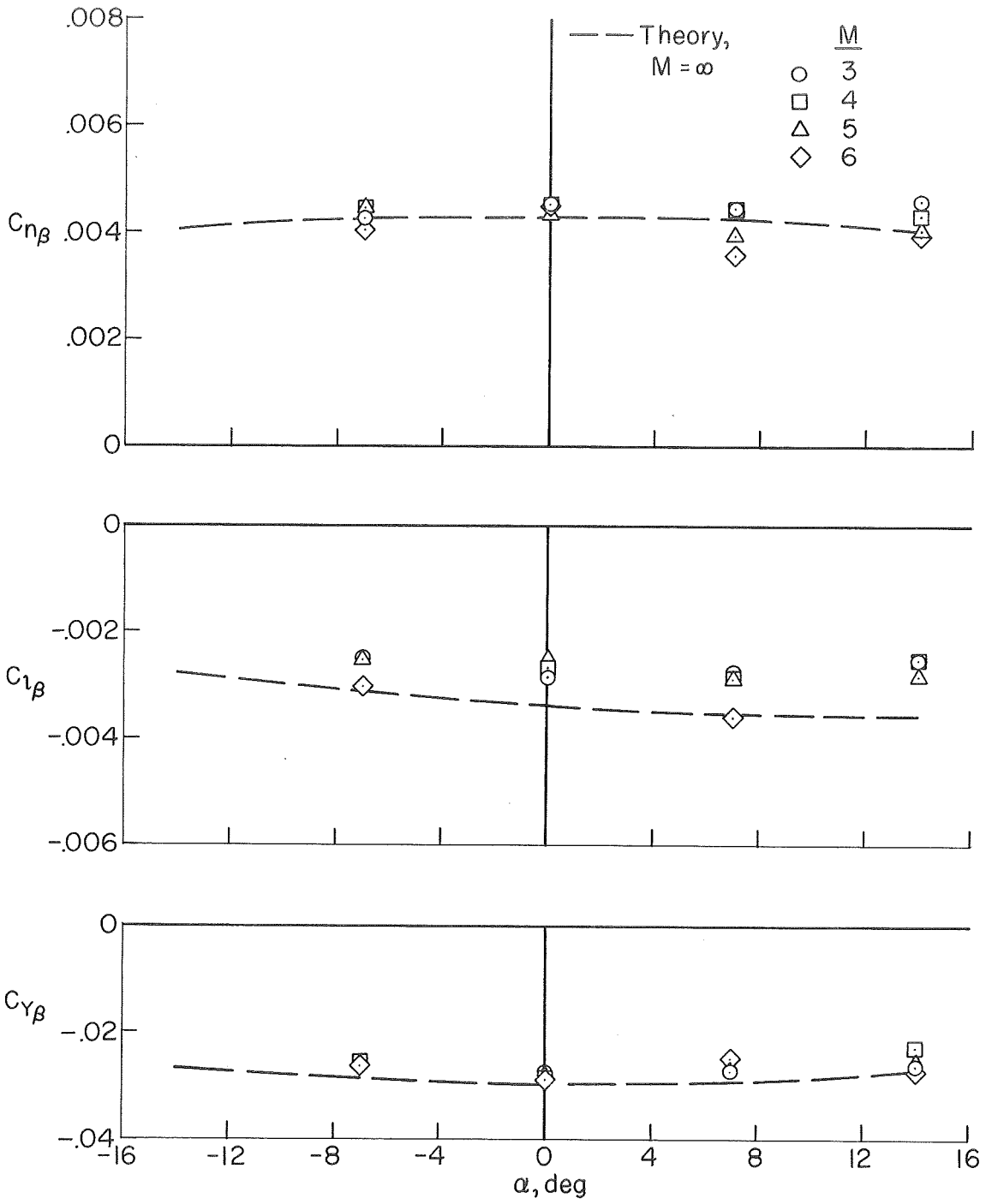

Figure 8.- Static stability of the study configuration; control set I undeflected.

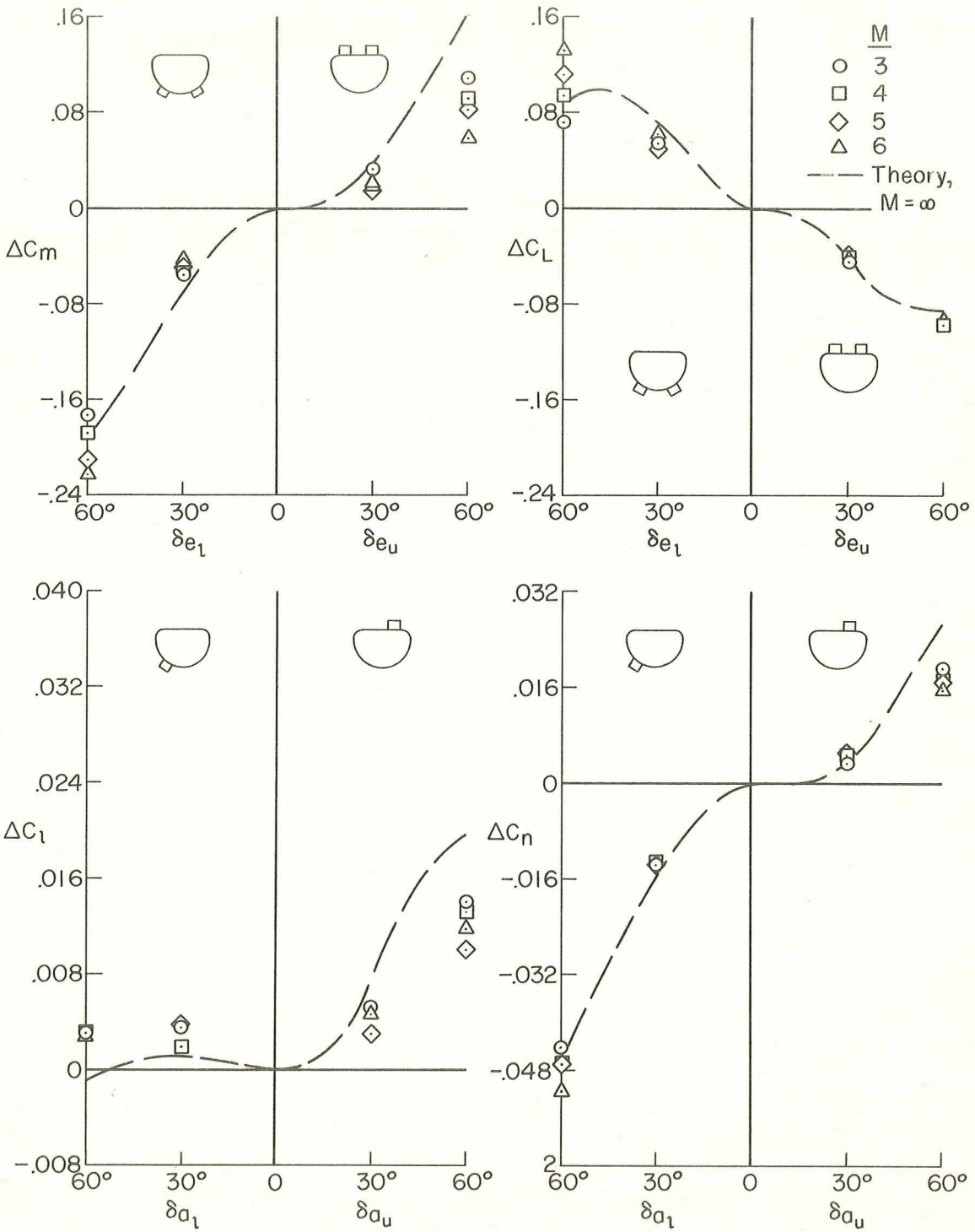

Figure 9.- Control characteristics at $\alpha = 0^{\circ}$; control set I.

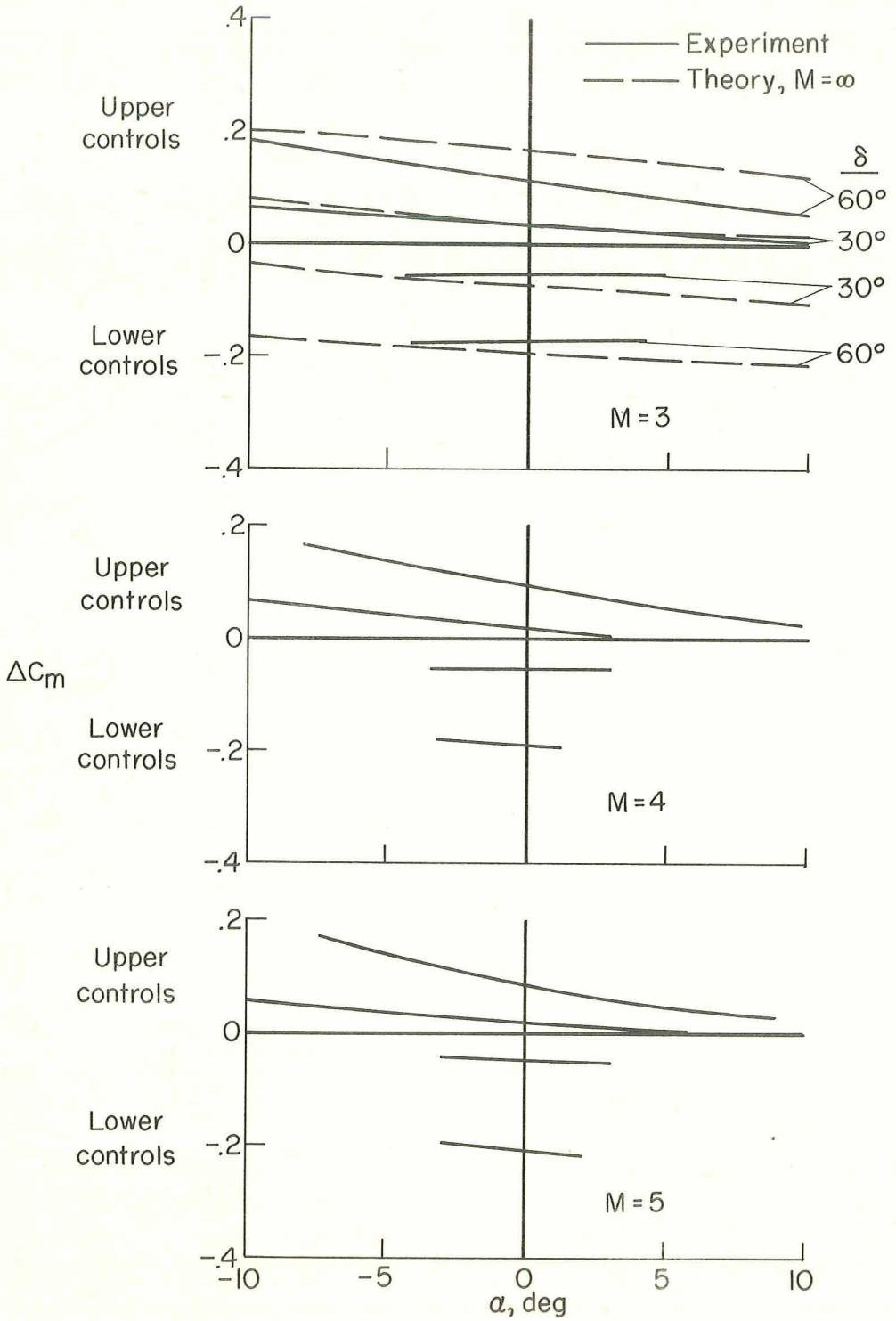

Figure 10.- Variation with angle of attack of the pitching-moment contribution due to control deflection; control set I.

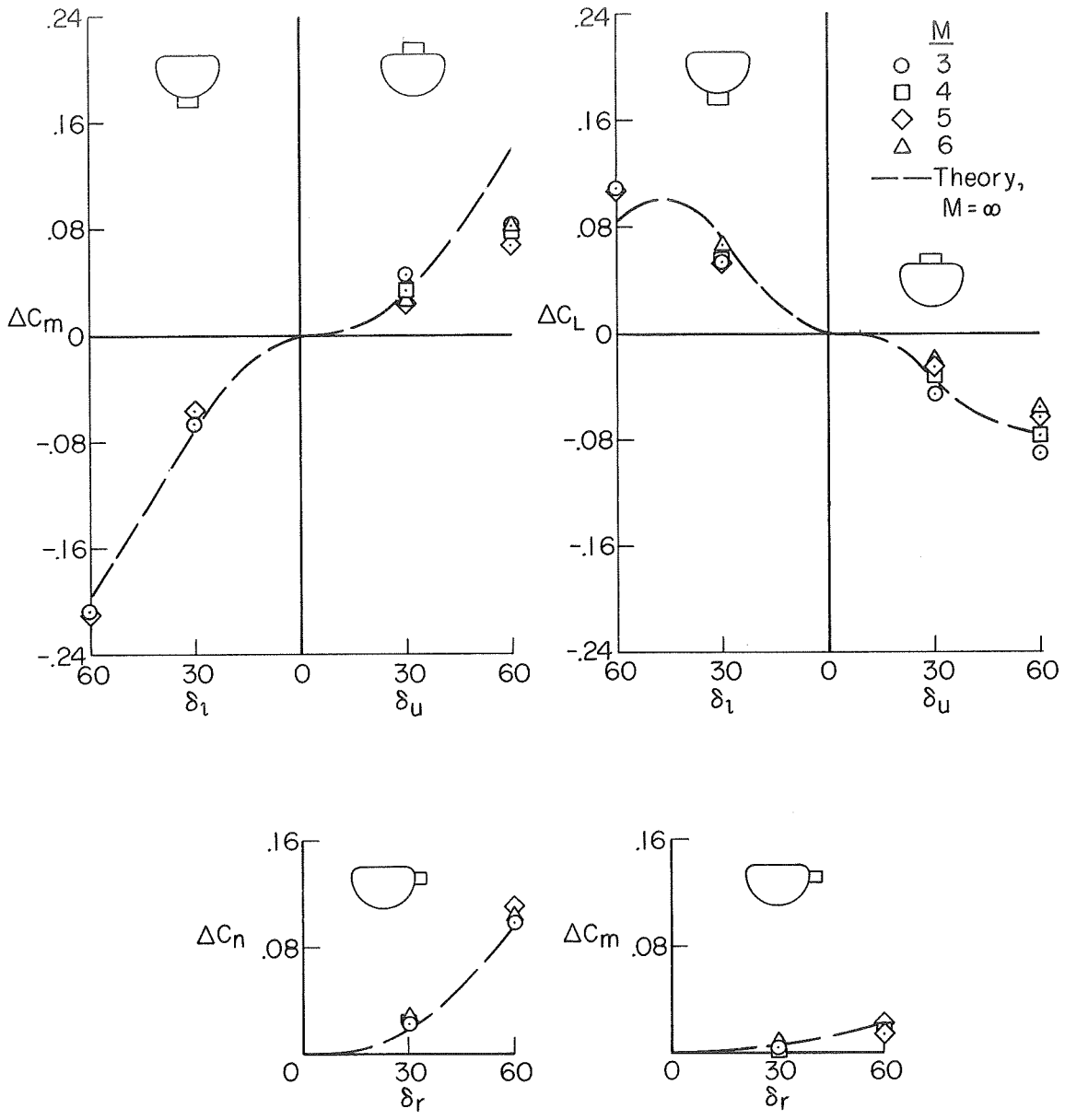

Figure 11.- Control characteristics at $\alpha = 0^{\circ}$; control set II.

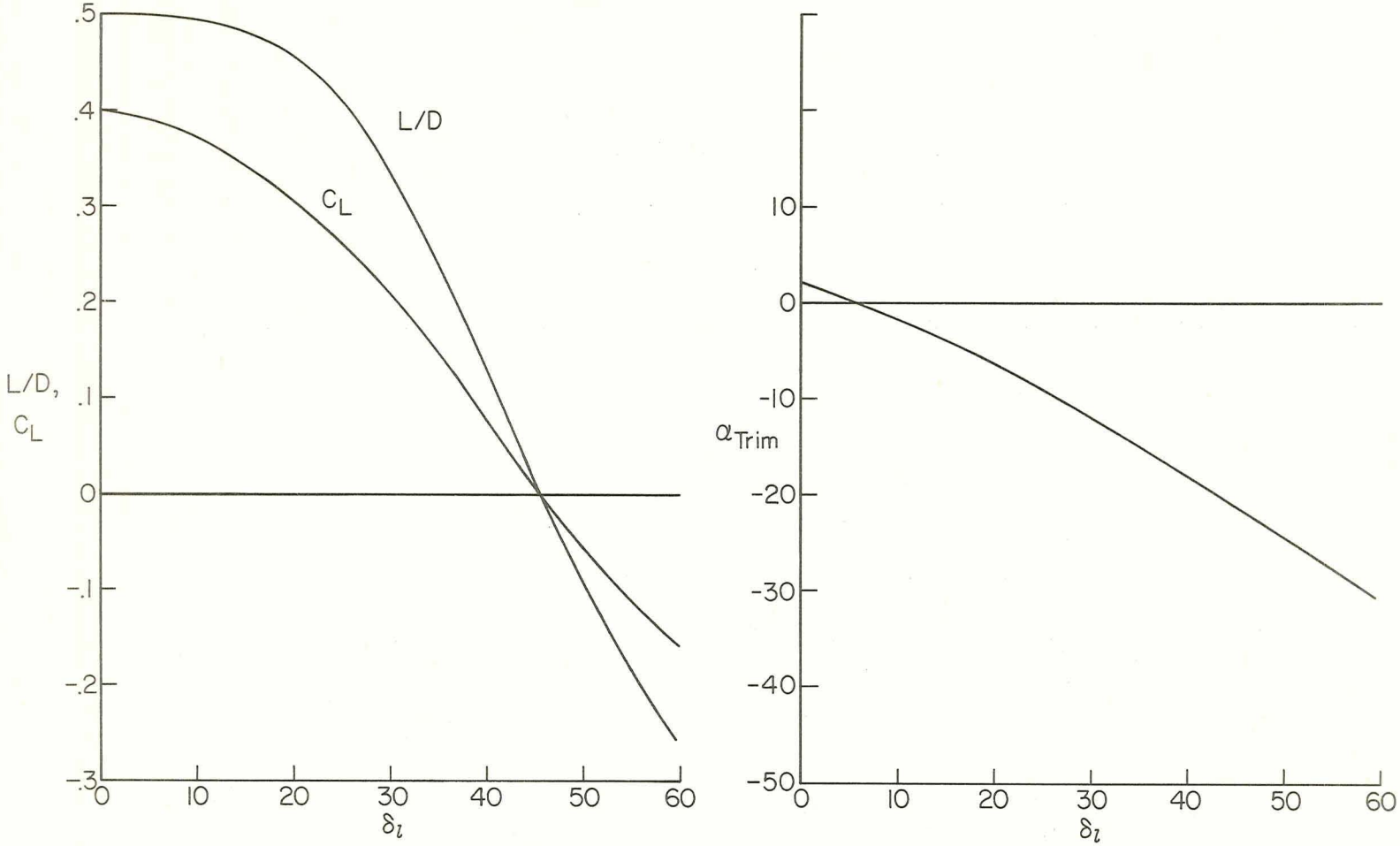

(a) Angle-of-attack variation; $\delta_u = 0^\circ$, $\delta_r = 0^\circ$.

Figure 12.- Estimated variation of trimmed lift-drag ratio with control deflection; control set II.

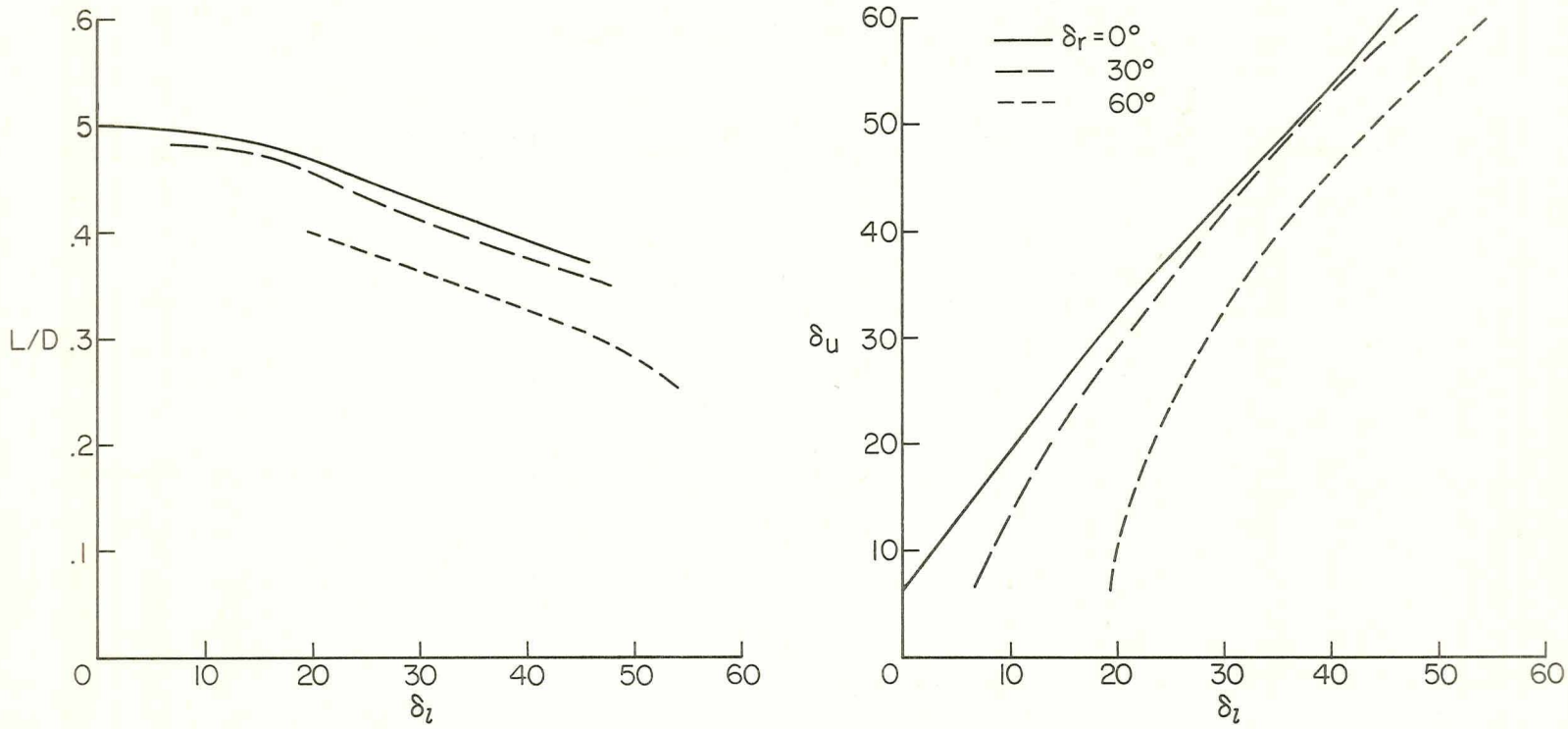

(b) All four controls used as drag brakes; $\alpha = 0^{\circ}$.

Figure 12.- Concluded.

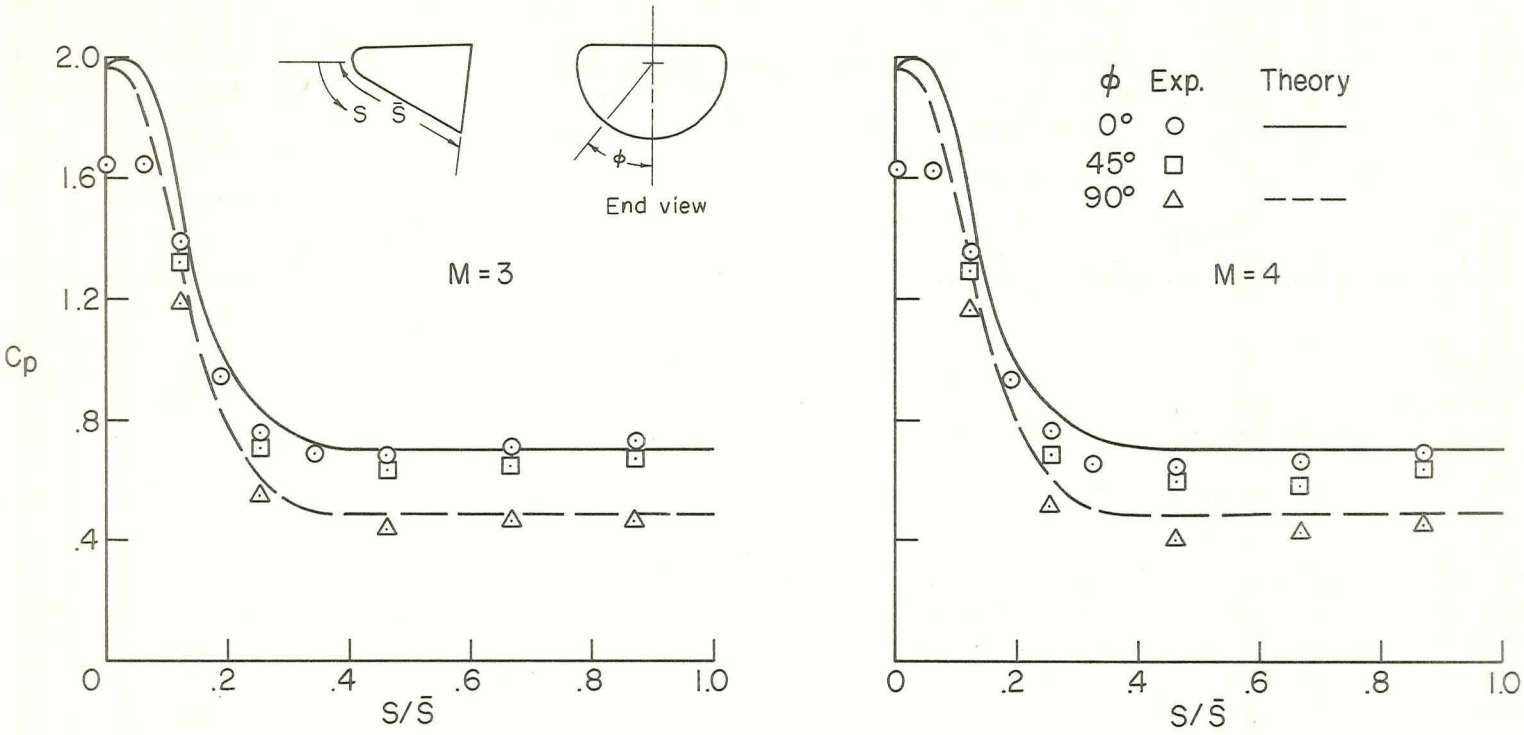

(a) Lower surface; M = 3 and 4.

Figure 13.- Pressure distribution on the study configuration; $\alpha = 0^{\circ}$.

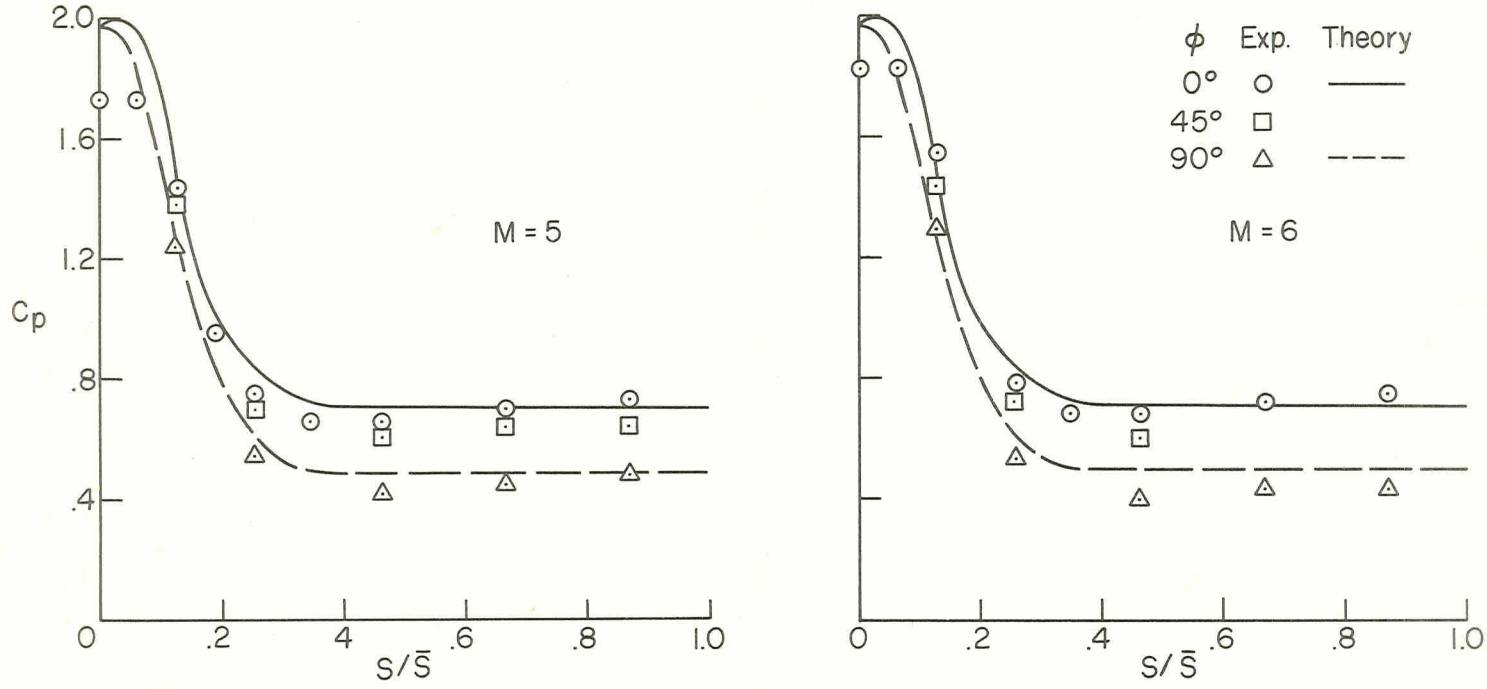

(b) Lower surface; M = 5 and 6.

Figure 13.- Continued.

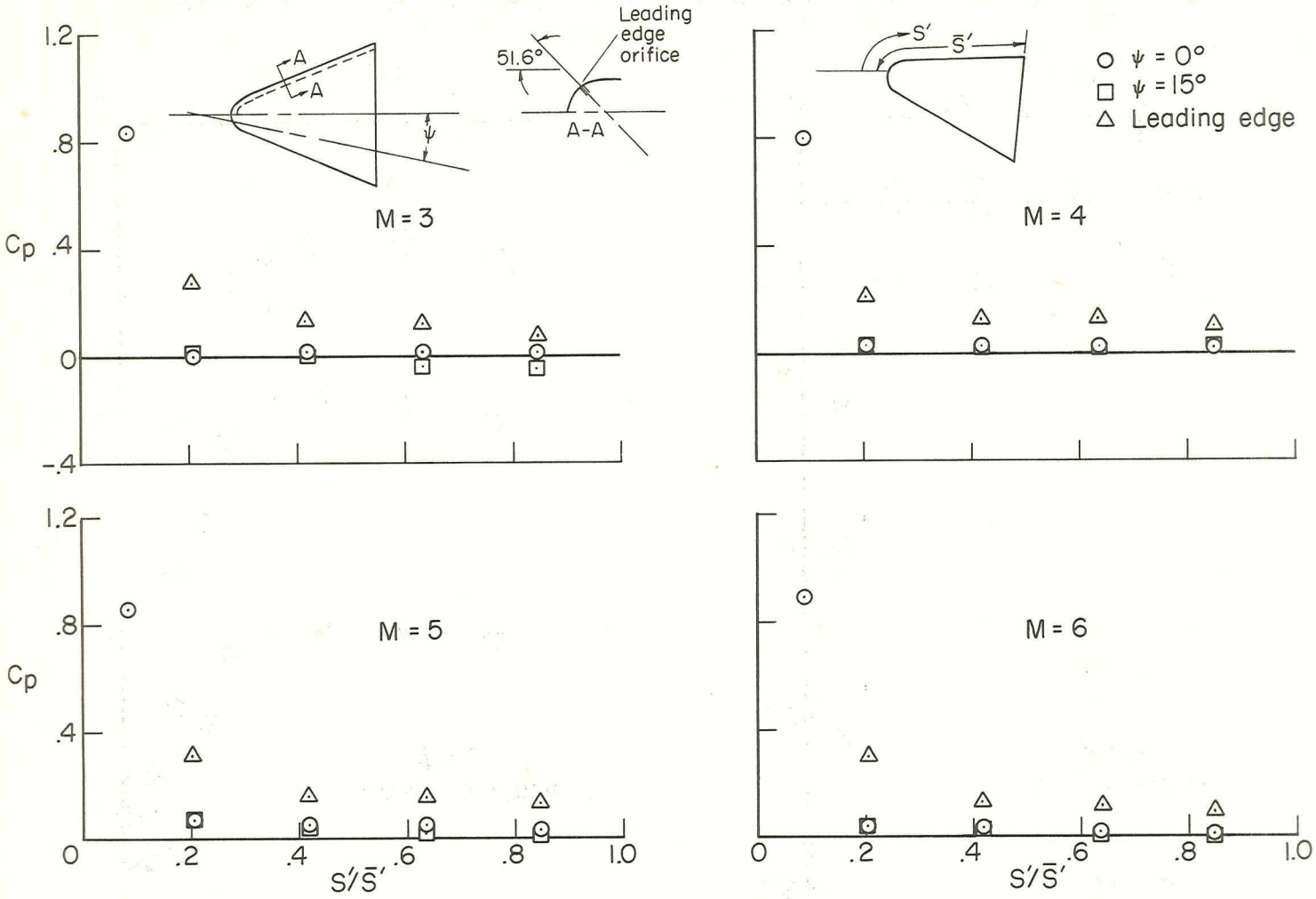

(c) Upper surface.

Figure 13.- Concluded.

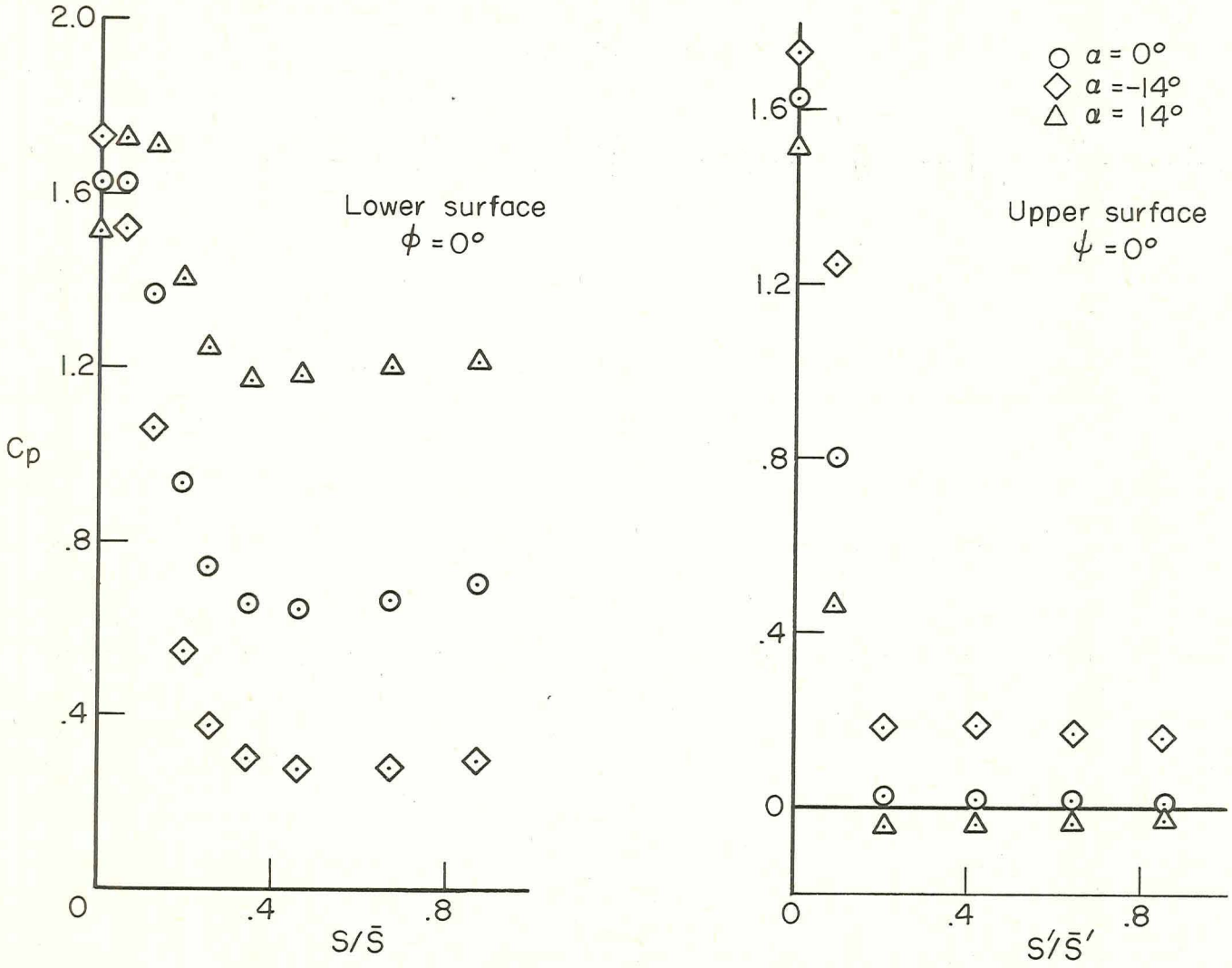

Figure 14.- Effect of angle of attack on body pressures at M = 4.

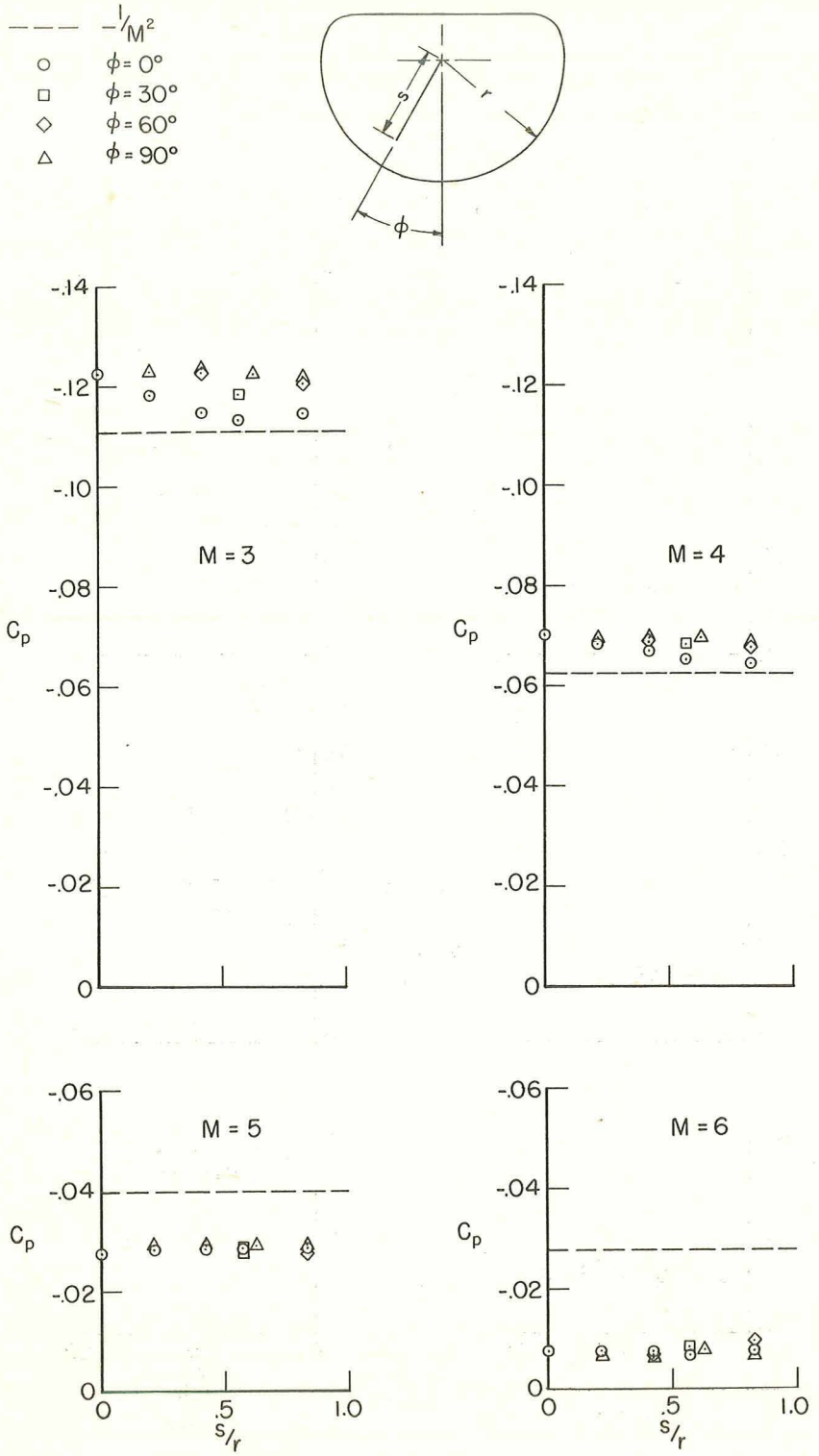

Figure 15.- Base pressure at $\alpha = 4°$.

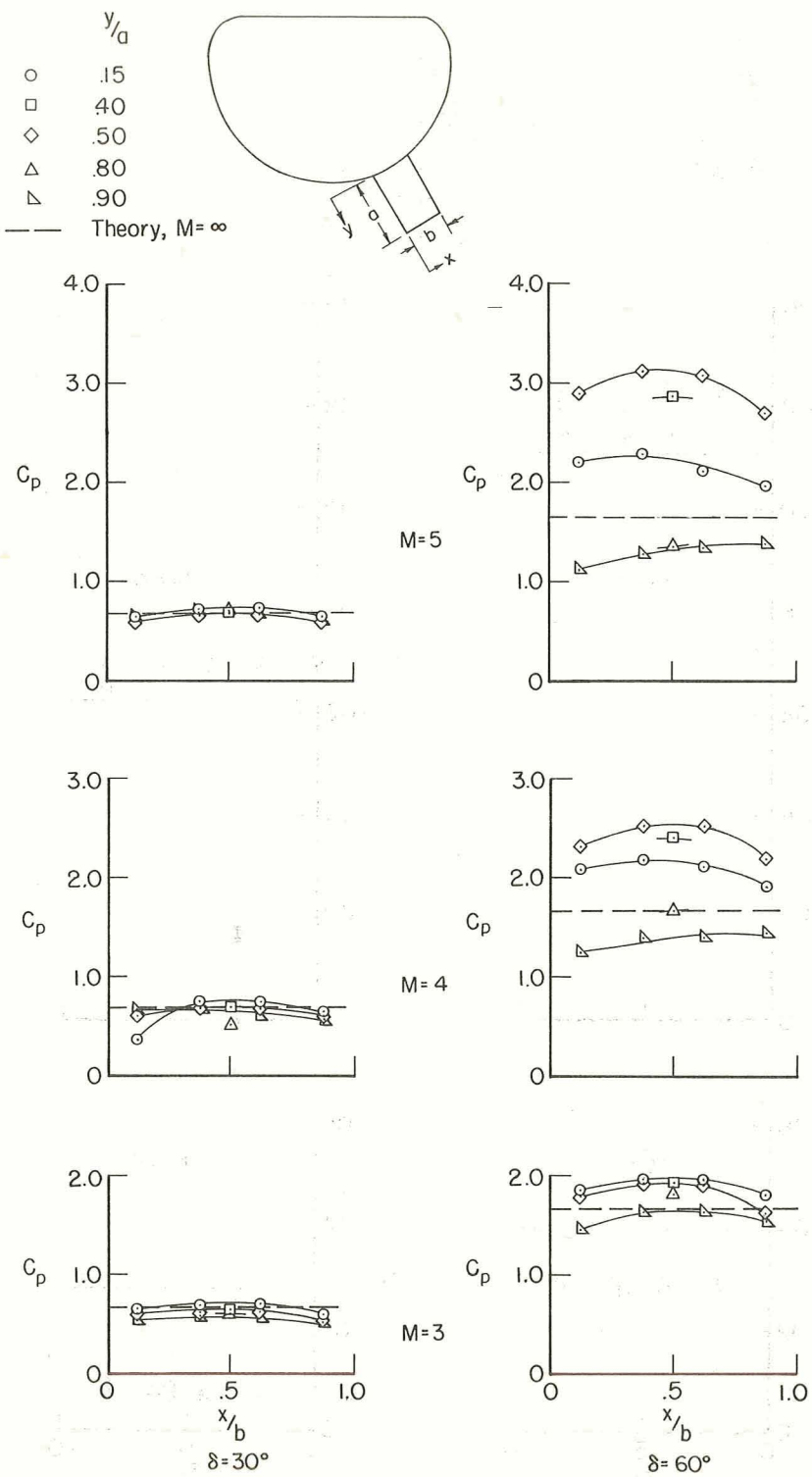

Figure 16.- Lower control pressure distribution; control set I, $\alpha = 0^{\circ}$.

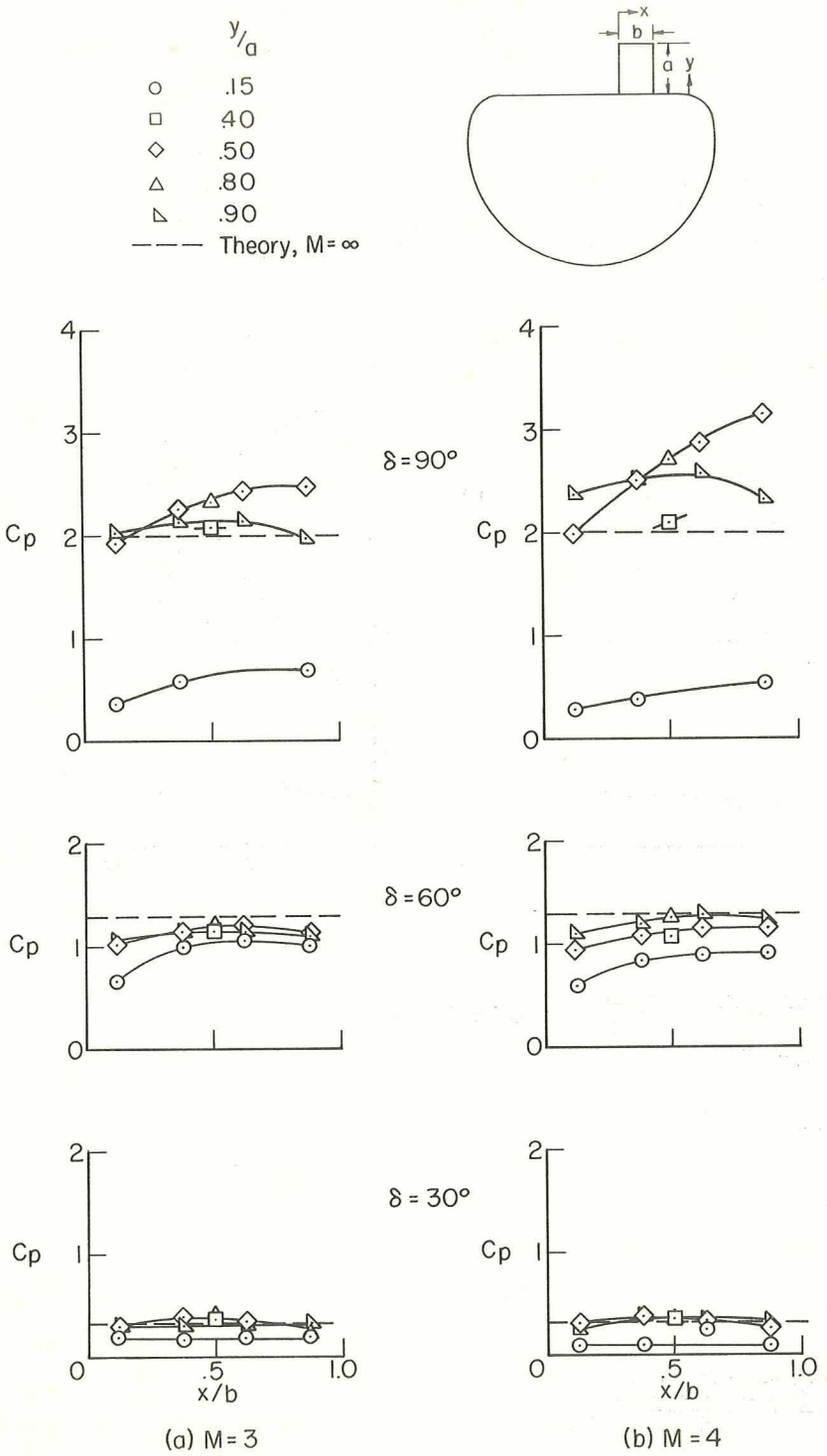

Figure 17.- Upper control pressure distribution; control set I, $\alpha = 0^{o}$.

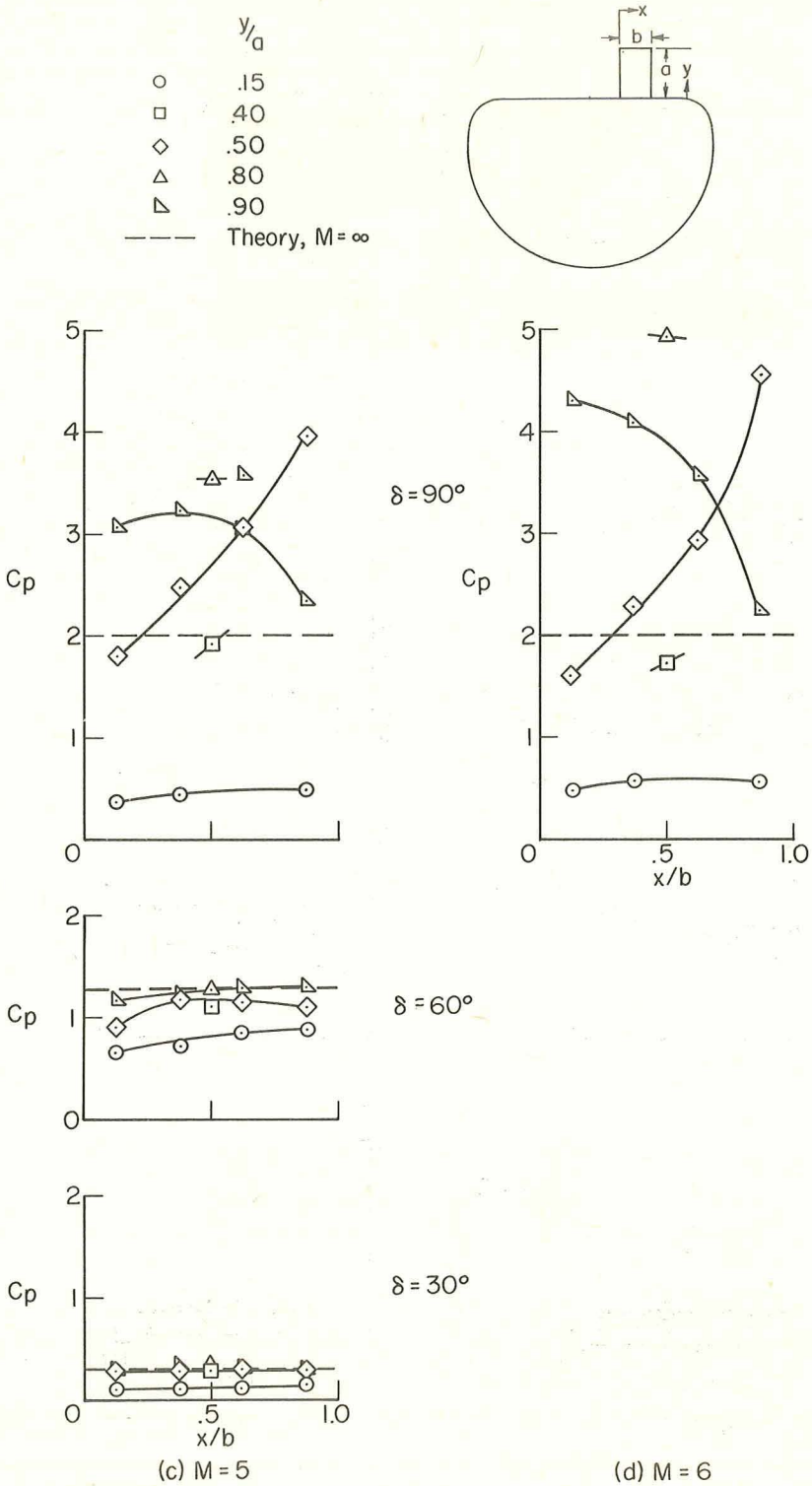

Figure 17.- Concluded.

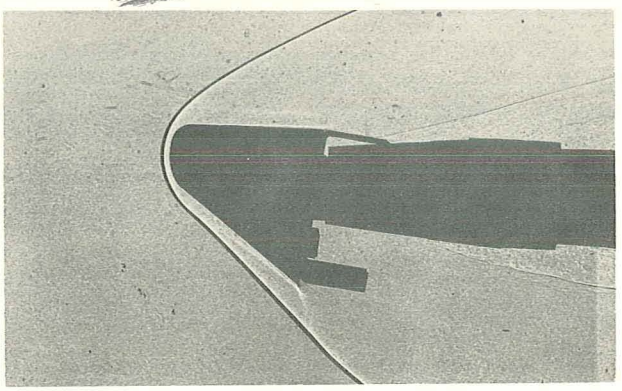

A-25648

(a) Study configuration controls undeflected; control set I, M = 3.

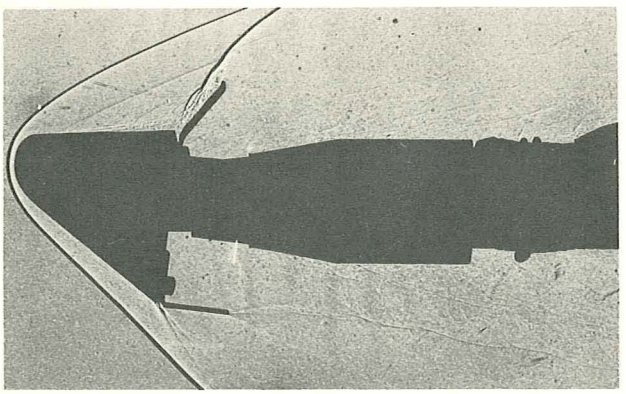

A-25650

(b) Upper control deflected 60° lower control undeflected; control set II, M = 4.

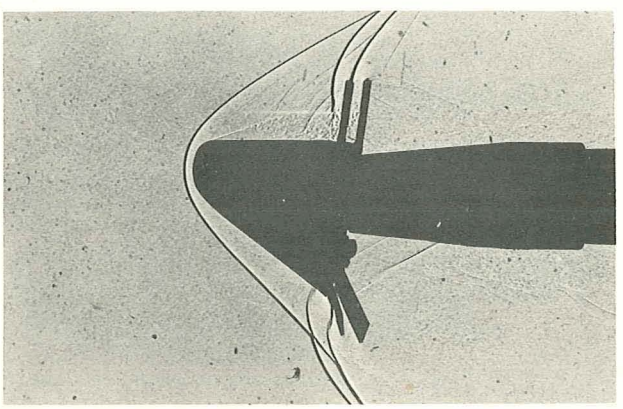

A-25649

(c) Upper controls deflected 90° lower controls 65°; control set I, M = 3.

Figure 18.- Shock-wave pattern on the study configuration.